eTransportation 20 (2024) 100314

Contents lists available at ScienceDirect

eTransportation

journal homepage: www.journals.elsevier.com/etransportation

# Urban-scale energy matching optimization with smart EV charging and V2G in a net-zero energy city powered by wind and solar energy

Reza Fachrizal [a,*,1], Kun Qian [b,1], Oskar Lindberg [a], Mahmoud Shepero [a], Rebecca Adam [b], Joakim Widén [a], Joakim Munkhammar [a]

[a] Built Environment Energy Systems Group (BEESG), Division of Civil Engineering and Built Environment, Department of Civil and Industrial Engineering, Uppsala University, Uppsala, Sweden

[b] Centre for Industrial Electronics (CIE), Department of Mechanical and Electrical Engineering, University of Southern Denmark, Sønderborg, Denmark

ARTICLE INFO

*Keywords:*
Electric vehicle smart charging
Vehicle-to-grid
Solar energy
Wind energy
Urban energy system
Net-zero energy

ABSTRACT

Renewable energy and electric vehicles (EVs) are crucial technologies for achieving sustainable cities. However, intermittent power generation from renewable energy sources and increased peak load due to EV charging can pose technical challenges for the power systems. Improved load matching through energy system optimization can minimize these challenges. This paper assesses the optimal urban-scale energy matching potentials in a net-zero energy city powered by wind and solar energy, considering three EV charging scenarios: opportunistic charging, smart charging, and vehicle-to-grid (V2G). A city on the west coast of Sweden is used as a case study. The smart charging and V2G schemes aim to minimize the mismatch between generation and load, and are formulated as quadratic programming problems. The simulation results show that the optimal load matching performance is achieved in a net-zero energy city with the V2G scheme and a wind-PV electricity production share of 70:30. The load matching performance in the optimal net-zero energy city is increased from 68% with opportunistic charging to 73% with smart charging and further to 84% with V2G. It is also shown that a 2.4 GWh EV battery participating in the V2G scheme equals 1.4 GWh stationary energy storage in improving urban-scale load matching performance. The findings indicate that EVs have a high potential to provide flexibility to urban energy systems.

## 1. Introduction

Cities are a major contributor to global $CO_2$ emissions, accounting for over 70% [1]. A large share of urban $CO_2$ emissions comes from the energy and transport sectors, which have mainly been relying on fossil fuels since decades ago [1]. In urban energy systems, the net-zero energy district or city concept has recently been promoted globally [2,3]. In a net-zero energy city, the city generates as much energy as it consumes, and the energy generated should come from renewable energy sources (RES), such as solar photovoltaic (PV) and wind energy [2]. With a net-zero energy city, the $CO_2$ emission challenges from city energy use are expected to be addressed [3,4]. To de-carbonize the urban transport sector, the transition towards electromobility has been promoted in recent decades [5]. It is important to note that using electric vehicles (EVs) for transportation can only be as environmentally friendly as its fuels [6,7]. This highlights the increased importance of deploying RES as transport electrification increases. In other words, both the integration of distributed renewable energy sources and electric transportation in the urban environment are considered crucial for future sustainable cities [5,8].

However, both integration of intermittent RES, such as wind and solar PV, and transport electrification create new technical challenges in the power system [9–11]. The shift to EVs in the transportation sector introduces new electricity demands in the power system which can lead to system overload [12,13]. On the other hand, the high penetration of wind and solar PV, which are non-dispatchable sources, can lead to system overgeneration [11,14]. These conditions can cause several power system issues such as voltage and frequency fluctuations, transformer and cable overloading, and increased energy losses in the system [10,11,15]. If these problems are not appropriately addressed, the costly and time-consuming power grid reinforcement may become necessary [16].

* Corresponding author.
*E-mail addresses:* reza.fachrizal@angstrom.uu.se (R. Fachrizal), kqian@sdu.dk (K. Qian), oskar.lindberg@angstrom.uu.se (O. Lindberg), mahmoud.shepero@angstrom.uu.se (M. Shepero), rebeccaadam@sdu.dk (R. Adam), joakim.widen@angstrom.uu.se (J. Widén), joakim.munkhammar@angstrom.uu.se (J. Munkhammar).

[1] These authors contributed equally to this work.

https://doi.org/10.1016/j.etran.2024.100314
Received 28 April 2023; Received in revised form 14 December 2023; Accepted 17 January 2024
Available online 18 January 2024

## Nomenclature

### Abbreviations

| | |
|---|---|
| BESS | Battery energy storage system. |
| CF | Capacity factor. |
| EV | Electric vehicle. |
| P/L | Production-to-load. |
| PV | Photovoltaic. |
| RES | Renewable energy sources. |
| RHC | Receding horizon control. |
| SC | Self-consumption. |
| SCSB | Self-consumption-sufficiency balance. |
| SS | Self-sufficiency. |
| V2G | Vehicle-to-grid. |

### Variables

| | |
|---|---|
| $\mathbf{A}$ | Auxiliary matrix to compute the cumulative sum. |
| $\mathbf{c}_e$ | The aggregated number of connected EVs at the end of each time. |
| $\mathbf{c}_p$ | The aggregated number of connected EVs during each time. |
| $\mathbf{e}_{agg}$ | The aggregated energy balance at each time (kWh). |
| $\mathbf{e}_a$ | The aggregated energy demand for those arriving at each time (kWh). |
| $\mathbf{E}_d$ | Auxiliary matrix denoting the aggregated energy demand by the departing time index for the arrived EVs at each time (kWh). |
| $\mathbf{e}_d$ | The aggregated energy demand for those departing at each time (kWh). |
| $\mathbf{n}_a$ | The aggregated number of arrivals at each time. |
| $\mathbf{n}_d$ | The aggregated number of departures at each time. |
| $\mathbf{p}_{agg}$ | Total aggregated charging/discharging power at each time (kW). |
| $\mathbf{p}_{cons}$ | Total power consumption at each time (kW). |
| $\mathbf{p}_{fix}$ | Total charging power for the inflexible sessions at each time (kW). |
| $\mathbf{p}_L$ | Total base load at each time (kW). |
| $\mathbf{p}_{opp}$ | Total charging power for the flexible sessions when applying "opportunistic" charging at each time (kW). |
| $\mathbf{p}_{prod}$ | Total power production at each time (kW). |
| $\mathbf{p}_{RES}$ | Total RES generation at each time (kW). |
| $\mathbf{p}_{sc}$ | Total charging power for the flexible sessions when applying smart charging at each time (kW). |
| $\mathbf{p}_{v2g}$ | Total charging power for the flexible sessions when applying smart charging and V2G at each time (kW). |
| $\mathbf{T}_d$ | Auxiliary matrix denoting the aggregated departing time index for the arrived EVs at each time. |
| $\phi_{P/L}$ | Production-to-load ratio (p.u.). |
| $\phi_{SCSB}$ | Self-consumption-sufficiency balance (p.u.). |
| $\phi_{SC}$ | Self-consumption (p.u.). |
| $\phi_{SS}$ | Self-sufficiency (p.u.). |
| $\tau$ | Temporal resolution (15 min). |
| $e$ | The energy demand of a charging session |
| $E_{EV,max}$ | Maximum stored energy in an EV (kWh). |
| $E_{EV,min}$ | Minimum stored energy in an EV (kWh).(kWh). |
| $K$ | Maximum number of time slots for the stay time. |
| $k$ | Time index $k \in \{1, \dots, K\}$. |
| $M$ | Total number of time slots in a year (35 040). |
| $P_{EV,max}$ | Maximum charging/discharging power for an EV (kW). |
| $P_{EV,min}$ | Minimum charging/discharging power for an EV (kW). |
| $t_a$ | The arrival time of a charging session. |
| $t_d$ | The departure time of a charging session. |

The challenges coming from RES and EV integration can be mitigated by improving the synergy between the two [17]. Deploying battery energy storage systems (BESS) is a straightforward way to improve the synergy between RES and the EV charging load or any load in general. However, BESS deployment is costly and can be economically infeasible in many cases [18]. The generation-load synergy can also be improved by utilizing flexible demand and generation units [17]. With long uninterrupted parking duration, EVs can act as flexible demand and generation units. It is possible to shift the charging load through smart charging control, or even discharge the energy from the EV batteries to the electricity grid or through vehicle-to-grid (V2G) control [17,19,20]. Similarly to why wind and solar energy are considered as intermittent RES, EV batteries participating in V2G schemes can be considered as intermittent energy storage, since EVs with V2G schemes are not constantly available and predictable as stationary energy storage for the power grid due to EV users' mobility behaviors. With these schemes, the optimal operation to improve the synergy between RES and EVs can be achieved without compromising user convenience, such as having a full battery by the time of departure [17].

Besides optimal operation, the sizing of RES in comparison to the load is also crucial. With oversized or undersized RES, the synergy between RES and EVs will remain sub-optimal, despite the deployment of smart charging schemes [21]. In order to realize sustainable urban energy and transport systems, it is important to implement both optimal operation and sizing of combined RES-EV systems in different parts of the built environment as well as at the city level as a whole. On the generation side, the optimal shares between different RES can help the energy systems achieve optimal load matching. For example, in mid-latitudes, wind electricity production typically peaks during the night on a diurnal basis and during winter on a seasonal basis, while PV electricity production peaks during the day on a diurnal basis and during summer on a seasonal basis [22,23]. With the complementary nature of wind and solar power generation, combining the two with the right shares will result in optimal load matching.

### 1.1. Related work and motivation

Net-zero energy systems have been a major research topic in the energy system field in recent years [24]. As previously mentioned, in a net-zero energy system, the system locally supplies as much renewable energy as it uses on an annual basis, meaning the ratio of local RES production to consumption is one [25]. Recent research has studied net-zero energy in different levels of the energy systems, for example at residential buildings [25,26], at commercial buildings [27,28], for electric mobility [29], on a community level [30,31], on a district level [3], and on a city-scale level [32]. It should be noted that a net-zero energy system may experience unfavorable power mismatches between consumption and production since it only considers the annual energy balance, not the instantaneous power matching. As previously mentioned, the lack of synergy between power consumption and production is one of the main sources of problems in the power grid [33].

Options for improving the synergy between local RES and load have also been a major research topic in recent years [33,34]. These include studies on the optimal operation and optimal sizing of renewable-powered energy systems considering EV flexibility utilization and different types of RES [35–37]. A considerable amount of research on

smart charging and V2G considering renewable generation to achieve optimal operation has been conducted in recent years.

Studies on PV-EV synergy through smart charging in different parts of the built environment, e.g., residential and workplace areas, have been more common than studies on wind-EV, since in such cases it is easier to integrate PV than wind power, e.g., on building rooftops [17]. Several research studies have investigated the EV smart charging and/or V2G impacts on the PV-EV synergy in different parts of the built environment, for example at residential areas [35,38–40], at workplace areas [21,41,42], on aggregator/charging station levels [43,44], on distribution grid levels [9,45,46], and on regional levels [47,48]. The improved synergy of PV-EV leads to an improved grid hosting capacity for both PV and EVs, as shown in [9] for a case study in Sweden, and in [45] for a case study in the U.K.

Studies on EV smart charging and V2G involving wind power have been more common on higher system levels, such as aggregator levels, rather than individual building levels. Studies on EV fleet charging scheduling considering wind power were presented in [37,49,50]. Several studies also considered both wind and PV for coordinated EV charging/discharging schemes to improve technical, economic, and environmental performances, such as in [51,52]. In [51], it was shown that the hosting capacity for wind and PV could be increased up to 20% with the deployment of EV smart charging schemes. Ref. [52] showed that implementing V2G schemes in power grids with high penetration of wind and PV improves grid reliability.

As mentioned previously, besides optimal operation, optimal sizing also plays an important role in improving the synergy between RES and EVs, and generation and load in general. A study in [21] proposed a novel technical measure, combining the self-consumption (SC) and self-sufficiency (SS) measures, to define the optimal sizing of PV-EV sizes at workplace charging stations. The mentioned study also concluded that the measure can be used to define the optimal RES-EV or generation-load sizing in general, in different parts of the built environment or on city-scale levels, as conducted in [53–55]. Previous research has also studied optimal RES sizing considering EV charging demand based on other measures, e.g., cost, as conducted in [28,31,44]. Studies on the optimal deployment of public EV charging stations, which involve sizing and placement, have also been conducted in previous research. Examples of such studies can be found in [54,56]. Research on the sizing of different RES sources, such as wind and PV, in the power systems to achieve optimal system performance has also been conducted in recent works. For example, Ref. [57] attempted to find the optimal share of wind and PV plant size to smooth the combined generation profile in a hybrid park. In [58], optimization of wind-PV plant share to reduce grid burden was presented.

Based on the literature review conducted in this study, it is clear that assessments of built environment energy system performance considering different variables are highly relevant. To the best knowledge of the authors, assessments of the urban-scale load matching potential considering different wind-PV electricity production shares, RES-load ratios, and degrees of EV flexibility utilization simultaneously have not been previously studied. In addition, an assessment on the technical value of EV flexibility as intermittent storage for urban-scale energy systems is also relevant and has not been conducted previously.

Studying EV scheduling in the context of urban-scale energy systems is a complex problem, given that traditional methods tend to solve the charging scheduling for each individual EV. These methods face increasing complexity due to the huge amount of decision variables resulting from the many EVs. For example, the load matching objective in [35] results in a quadratic programming problem, and the complexity suffers from a polynomial increase with an increasing number of variables [59]. Moreover, studies focusing on providing accurate scheduling for EVs consider practical constraints such as minimum charging power [60], which can result in integer decision variables, leading to an exponential increase in the computational complexity [61]. However, for energy system evaluations, the overall EV charging load is of interest rather than the scheduling for each EV. Ref. [62] proposed an aggregated model that directly solves the overall EV charging load, which has fixed complexity since the number of EVs does not affect the number of decision variables. The aggregated model has been further simplified and validated in [55].

### 1.2. Contribution

This paper complements previous research and contributes to the field by assessing the optimal load matching of urban energy systems considering EV flexibility and renewable energy deployment. The study utilizes the aggregated EV model validated in [55]. Table 1 summarizes the comprehensive comparison between the literature reviewed and the study in this paper based on four key aspects: studied systems, RES supply, EV flexibility, and energy system optimization. This study specifically focuses on the electricity needs of urban energy systems, including transport electrification. The impacts of smart EV charging and V2G on urban energy systems are assessed in this study. This study uses the urban mobility and energy system of a Swedish city as a case study. The main contribution of this paper lies in its thorough investigation of the following topics:

1. The optimal wind-PV and RES generation-load sizing to reach optimal load matching performance in city-scale energy systems considering three different EV charging scenarios, i.e., opportunistic charging, smart charging, and V2G.
2. The potential of improved synergy between wind-PV generation and electricity consumption in a net-zero energy city by smart charging and V2G schemes.
3. The technical value of EV flexibility with V2G schemes as intermittent energy storage compared to traditional stationary energy storage.
4. The possibility of transforming a net-zero energy city into a self-sufficient energy city with different EV charging scenarios and stationary storage capacities.

The investigation was carried out through simulation studies. It should be noted that this study does not aim to propose or use scheduling methods for individual EV charging/discharging. Instead, as mentioned previously, a validated model to quantify the aggregated EV charging demand and discharging production, regardless of the charging strategy, will be used. In this study, this approach is adopted because the focus is on the overall EV charging load for energy system evaluation, rather than the scheduling of individual EVs.

### 1.3. Structure of the paper

The paper is structured as follows: In Section 2, the simulation data, assumptions, scenarios, models, and performance measures are described. Section 3 presents the simulation results related to the four topics investigated in this paper. In Section 4, the results and possible future works are discussed. Section 5 concludes the paper.

## 2. Methods

This section describes the methods used in this paper. Since the study focuses on optimizing urban-scale energy system balance, the studied scope is delimited within a higher energy system level. With this delimitation, this study does not include simulations for individual systems, for example individual EVs and buildings, and aggregate the simulation results afterwards. Instead, this study first models the aggregated representation of the systems and then performs simulations on the aggregated level. Fig. 1 illustrates the outline of the city electricity systems and the emphasis of the aggregated level of energy systems being the scope of the optimization.

The workflow of urban-scale energy system optimization conducted in this paper, which includes both optimal operation and sizing, is

**Table 1**
A comparative summary between previous works and this study in terms of studied energy systems, RES supply involved, EV charging flexibility, and energy system optimization.

| Ref. | Studied systems | | RES supply | | EV charging flexibility | | | Energy system optimization | |
|---|---|---|---|---|---|---|---|---|---|
| | Net-zero energy | Urban-scale level | Solar PV | Wind | Opportunistic charging | Smart charging | V2G | Optimal operation | Optimal sizing |
| [3] | ✓ | | ✓ | ✓ | ✓ | | | | ✓ |
| [9,38,41,42] | | | ✓ | | ✓ | ✓ | | ✓ | |
| [19] | | | | | ✓ | ✓ | ✓ | ✓ | |
| [21] | | | ✓ | | ✓ | ✓ | | ✓ | ✓ |
| [25] | ✓ | | ✓ | | | | | ✓ | ✓ |
| [26] | ✓ | | ✓ | | ✓ | ✓ | ✓ | ✓ | |
| [27] | ✓ | | ✓ | ✓ | | | | ✓ | ✓ |
| [28] | ✓ | | ✓ | | ✓ | ✓ | ✓ | ✓ | ✓ |
| [29] | ✓ | ✓ | ✓ | | ✓ | | | ✓ | ✓ |
| [30] | ✓ | | ✓ | | | | | ✓ | |
| [31] | ✓ | | ✓ | ✓ | ✓ | ✓ | ✓ | ✓ | ✓ |
| [32] | ✓ | ✓ | ✓ | | | | | | ✓ |
| [35] | ✓ | | ✓ | | ✓ | ✓ | | ✓ | |
| [36,48] | | ✓ | ✓ | | ✓ | ✓ | ✓ | ✓ | |
| [37] | | | | ✓ | ✓ | ✓ | | ✓ | ✓ |
| [39,40,43,45,46] | | | ✓ | | ✓ | ✓ | ✓ | ✓ | |
| [44] | | | ✓ | | ✓ | ✓ | ✓ | ✓ | ✓ |
| [52] | | | ✓ | ✓ | ✓ | ✓ | ✓ | ✓ | |
| [47] | ✓ | ✓ | ✓ | | ✓ | ✓ | ✓ | ✓ | |
| [49] | | | | ✓ | ✓ | ✓ | | ✓ | |
| [50] | | | | ✓ | ✓ | ✓ | ✓ | ✓ | |
| [51] | | | ✓ | ✓ | ✓ | ✓ | | ✓ | |
| [54] | | | ✓ | | ✓ | ✓ | ✓ | | |
| [56] | | ✓ | | | ✓ | ✓ | ✓ | ✓ | |
| [57] | | ✓ | ✓ | ✓ | | | | | ✓ |
| [58] | ✓ | | ✓ | ✓ | | | | | ✓ |
| **This study** | ✓ | ✓ | ✓ | ✓ | ✓ | ✓ | ✓ | ✓ | ✓ |

illustrated in Fig. 2. Three blocks representing the scope of the study are included in Fig. 2 which corresponds to: 1. data preparation, aggregation, and modeling, 2. EV charging modeling and optimal operation, and 3. optimal sizing of the urban energy systems. A more detailed analysis of urban energy matching performance and technical value of V2G will be conducted after the optimal system is defined. It should be noted that this work aims to evaluate the load matching potential of an existing energy system. Hence, historical data is directly used without considering uncertainty. With this assumption, the results represent the best-case approximation of urban-scale load matching potentials in the case study.

More detailed explanations of each study scope shown in Fig. 2 are presented in the following sections. Section 2.1 presents aggregated data and the assumptions used in the study. Section 2.2 presents how to validate and aggregate the charging sessions for later simulations. Both Sections 2.1 and 2.2 correspond to data preparation, aggregation, and modeling parts of the study. In Section 2.3, the aggregated smart charging and V2G optimization models and algorithm are specifically described, which corresponds to optimal operation part of this study. Section 2.4 presents the energy matching measures used to assess the urban-scale energy performance. The simulation scenarios conducted in this study are presented in Section 2.5. Sections 2.4 and 2.5 are integral parts of the optimal sizing conducted in this study.

### 2.1. Data and case study

This section presents the data used in the study. More specifically, Section 2.1.1 presents the case study and data that is used to model the aggregated city power consumption and production. Section 2.1.2 presents the mobility data and the process for how to convert from travel sessions to charging sessions.

#### 2.1.1. City-scale electricity consumption and renewable power generation

The study uses real measured data from an electricity grid on the west coast of Sweden in 2021 from [22]. The electricity grid serves a city and some neighboring suburbs with an approximate population of 100,000. The maximum aggregated peak load is 94 MW and the annual electricity consumption is 372 GWh. The load is typical for the case of Sweden, with prominent seasonal variations with higher consumption in winter compared to summer.

The grid has 33 $MW_p$ of wind power, and 2.7 $MW_p$ of PV installed, respectively. These are measured on the aggregated level, meaning there are two production time series, one for the aggregated wind power output and one for the aggregated PV power output. The measured capacity factors of wind and PV power plants in this study are 0.35 and 0.14, respectively. Both wind and PV annual electricity production (MWh) are scaled up to match certain annual electricity demand levels (MWh), so that different city energy system scenarios can be simulated, for example, a scenario of a net-zero energy city with 50:50 wind-PV electricity production shares. Further details on simulation scenarios are presented in Section 2.5. It should be noted that even though the scope of the study is focused on the city-scale, the city energy system is still connected to the outer transmission grid. This implies that any power imbalance within the city is assumed to be handled by the transmission grid.

Both load and RES production data are originally in 10-min resolution. However, they were averaged to a 15-min resolution in order to match the resolution of the simulation setup intended for load matching assessment in this study. The use of 15-min resolution was motivated by the findings in [33,63], which showed that 15-min resolution was sufficient for a load matching assessment.

#### 2.1.2. Mobility patterns and charging sessions

This study utilizes the synthetically generated travel sessions from the model in [64], which relies on the Swedish travel survey [65]. The survey consists of information from the trips made by cars and other information which is representative for Swedish conditions. In the generated sessions, each travel session is associated with a unique user ID, and the travel sessions from the same user ID form the travel behavior for that user over the year. It is here assumed that all personal cars in the city are electric. For the specific Swedish city, depending on the population, personal car ownership percentage, and productive age percentage [66], this work assumes a total of around 37 000 users. With this assumption, the annual EV electricity demand (MWh) corresponds to 15% of the total annual electricity demand (MWh) in the city.

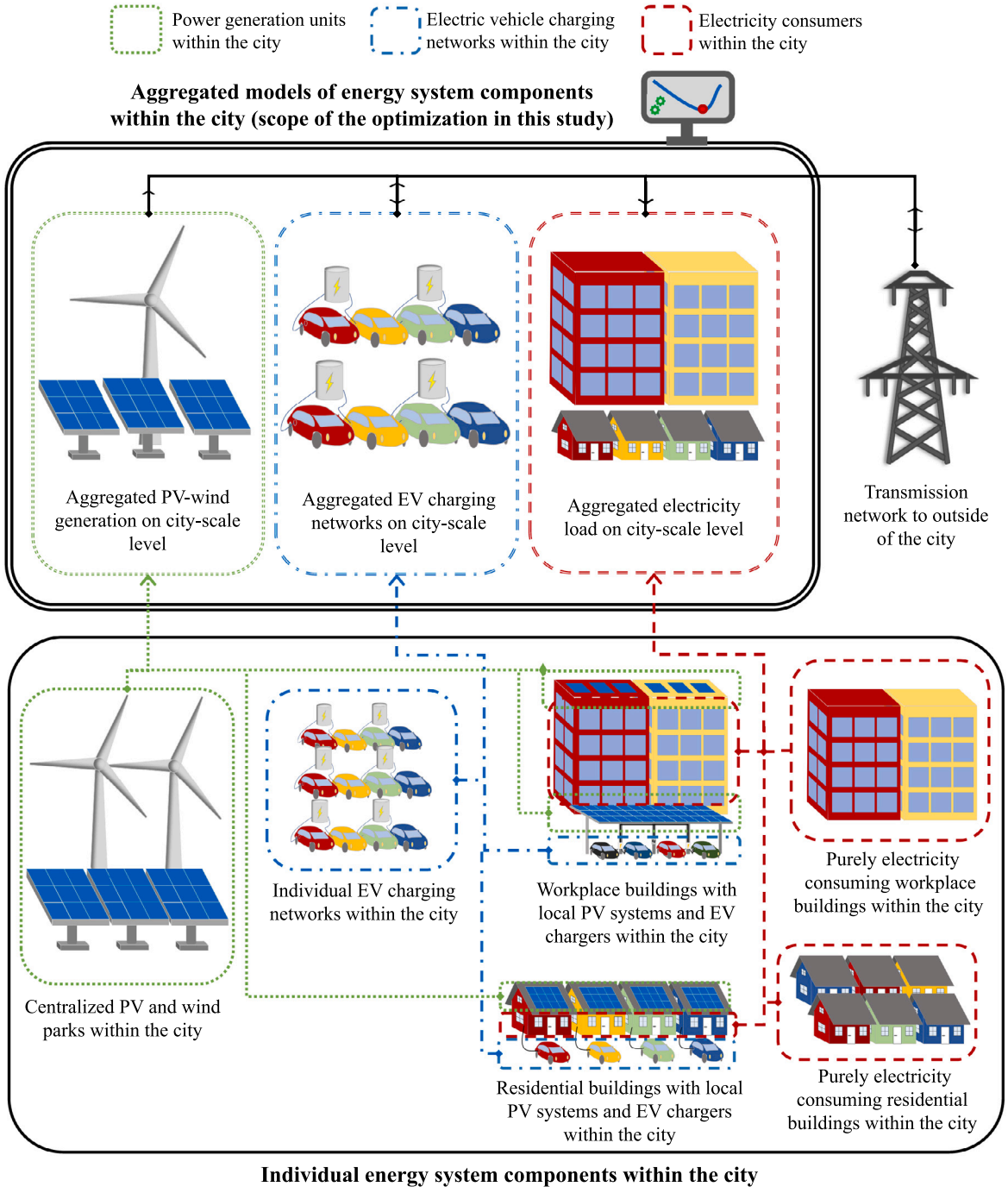


**Fig. 1.** The city electricity system outline simulated in this study. This figure highlights that the scope of the optimization in this study is on the aggregated level, not on the individual level.

Each travel session contains information: the user ID (UID), arrival time, arrival place, and consumed energy. The arrival time is a timestamp with a minute resolution. The arrival place is distinguishable by the place ID, which represents home, work, and other places. The consumed energy is computed from the driving distance with an assumption that 1 kWh equals 5 km driving distance, which conforms to the rates of many available EV models [67].

This work assumes that EVs charge either at home or at work, and the home-work charging ratio is 4 : 1 [68]. Correspondingly, 80% of users will charge at home while the rest are charging at work. Upon deciding whether the UID utilizes home or workplace charging, the travel sessions can be converted to charging sessions. A charging session is defined as a 4-tuple $(\mathrm{UID}, t_a, t_d, e)$, where $t_a$ is the arrival time index, $t_d$ is the departure time index, and $e$ is the energy demand. Note that in this study, an EV arrives at a time index means it arrives just before the time index while departing at a time index means the EV departs just after the time index.

The arrival times are the valid arrivals: after categorizing the UID in either home or workplace charging, the valid arrivals are those arriving at that location. Associated with each valid arrival, the next arrival in the travel sessions indicates the departure time (subtracting the driving time from that arrival, and this work assumes an average driving speed of 50 km/h, which is approximately the most economical driving speed that can reach the maximum remaining driving range [69]). The energy

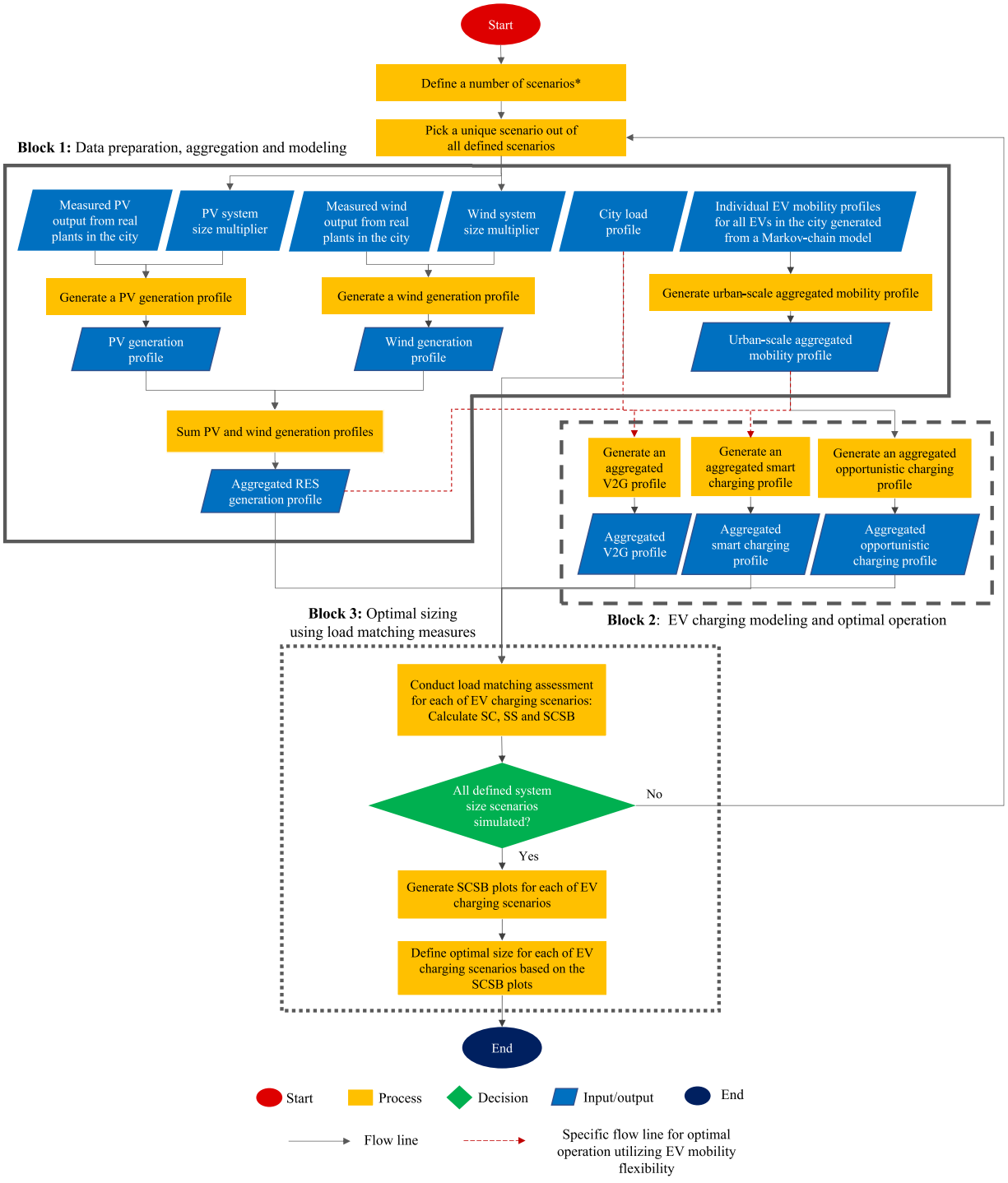


**Fig. 2.** Flowchart of the urban-scale energy system optimization conducted in this paper. * The conducted studies identified two optimal sizings: 1. Sizing of the wind-PV share of electricity, 2. Sizing of the aggregated RES-load ratio. In the wind-PV share sizing, the aggregated RES-load ratio was set to 1, representing a net-zero energy city scenario, and several wind-PV shares were simulated. In the aggregated RES-load ratio sizing, the wind-PV share ratio was set to the optimal wind-PV share obtained from the wind-PV optimal sizing, and several RES-load ratios were simulated.

demand is the accumulated energy use of the travel sessions from (but excluding) the previous valid arrival until the current valid arrival.

### 2.2. Validated charging sessions and aggregation

This section and the following section heavily depend on mathematical expressions, which include different constants and variables. For clarity, lowercase letters denote scale variables (e.g., $t_a$ denotes the arriving time of one EV); uppercase letters denote constant values (e.g., $P_{EV,max}$ denotes the maximum EV charging power); lowercase boldfaced letters denote vectors (e.g., $\mathbf{p}_{RES}$ denotes the RES generations at each time slot over the scheduling horizon), of which, the $i$th element can be indexed by $[\cdot]_i$; and uppercase boldfaced letters denote matrices (e.g., $\mathbf{A}$ denotes an auxiliary matrix, which will be described in detail later), of which, the element at $i$th row and $j$th column can be indexed by $[\cdot]_{i,j}$.

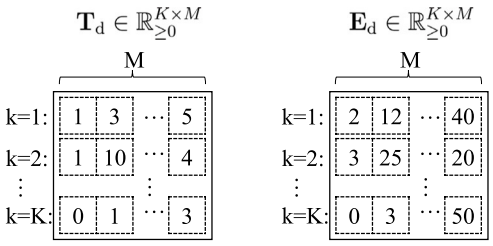


**Fig. 3.** Example $\mathbf{T}_d$ and $\mathbf{E}_d$ to illustrate the indication of the elements. For example, looking at $k = 2$ for $\mathbf{T}_d$, the example shows that for all those EVs arriving at $k = 2$, there are 1, 10, and 4 EVs departing after staying for one, two, and $M$ time slots, respectively. Correspondingly, looking at $k = 2$ for $\mathbf{E}_d$, the total required energies are 3 kWh (for 1 EV), 25 kWh (for 10 EVs), and 20 kWh (for 4 EVs) by the end of one, two, and $M$ time slots, respectively. Note that different EVs can have different energy demands.

Due to the decision time slot duration, the arrival and departure times are rounded up and down to the next valid time index, respectively. This can result in invalid charging sessions where the arrival time is later than the departure time. The departure times are set to the arrival times to avoid problems in the later simulations. This leads to another issue where the minimum required charging time (this work assumes maximum charging/discharging power at 11 kW) is longer than the stay duration. The unfulfilled energy demand must then be shifted until the next charging session. However, there is a maximum valid energy demand since this work assumes the same battery with the capacity 60 kWh, which has a minimum and maximum state-of-charge at 20% and 100% (as in [70]), respectively. Thus, the minimum and maximum energy in an EV battery are 12 kWh and 60 kWh, and the resulting maximum energy demand is 48 kWh. Those data processing steps are necessary to provide valid charging sessions.

Similar to [47,62], an aggregated model is applied. Compared to the individual model, the aggregated model can significantly reduce the model complexity and computation time. A few auxiliary vectors and matrices are provided to quantify the aggregated charging behavior based on the valid charging sessions.

There are two cases in the verified charging sessions: The minimum required charging time is equal to or smaller than the stay duration. For the sessions where the minimum required charging time equals the stay duration, the EV must charge during the whole stay, which leaves no flexibility. Otherwise, the extra stay time provides the potential for smart charging/discharging control.

This work considers a scheduling horizon over the year (365 days) with the decision time slot duration as $\tau = 15$ min, resulting in $K = 35\,040$ slots. To quantify the aggregated charging sessions, let $\mathbf{p}_{\text{fix}} \in \mathbb{R}_{\geq 0}^{K \times 1}$ denote the aggregated charging power from the inflexible charging sessions, and let $\mathbf{p}_{\text{opp}} \in \mathbb{R}_{\geq 0}^{K \times 1}$ denote the aggregated charging power from the flexible charging sessions where the EVs also charge upon arrival.

Additionally, for EVs arriving at time index $k$, let $\mathbf{T}_d \in \mathbb{R}_{\geq 0}^{K \times M}$ and $\mathbf{E}_d \in \mathbb{R}_{\geq 0}^{K \times M}$ denote the aggregated departing time index and the corresponding energy demand with $k$th row, where $M$ is the maximum number of slots for the stay time (According to the mobility behavior in this study, the maximum number of hours a car staying is 480 h, and thus, $M$ is 1920). Fig. 3 provides example $\mathbf{T}_d$ and $\mathbf{E}_d$ to better illustrate the construction of these two matrices.

Since the $k$th row of $\mathbf{T}_d$ captures the departing index of all the EVs arriving at time index $k$, applying summation over the row will result in the total number of EVs arriving at time index $k$. Thus, applying summation over all rows results in a vector, denoted by $\mathbf{n}_a \in \mathbb{R}_{\geq 0}^{K \times 1}$, which tells how many EVs arrive at each time index. To get how many EVs depart at each time index, denoted by $\mathbf{n}_d \in \mathbb{R}_{\geq 0}^{K \times 1}$, the summation will be applied to the column. However, before summation, it is necessary to convert $\mathbf{T}_d$ to $\mathbf{T}'_D \in \mathbb{R}_{\geq 0}^{K \times (M+K-1)}$ by shifting the

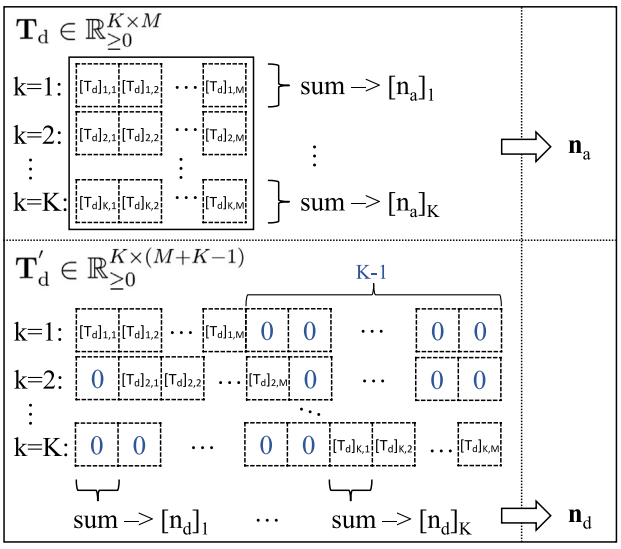


**Fig. 4.** Illustrating how to get $\mathbf{n}_a$ and $\mathbf{n}_d$ from the departing matrix $\mathbf{T}_d$. The $k$th element of $\mathbf{n}_a$ is the summation over the $k$th row of $\mathbf{T}_d$. The $k$th element of $\mathbf{n}_b$ is the summation over the $k$th column of $\mathbf{T}'_d$, which is a result from shifting the $k$th row to the right by $k - 1$ elements and patching $K - 1$ zeros at each row (as shown in blue color). (For interpretation of the references to color in this figure legend, the reader is referred to the web version of this article.)

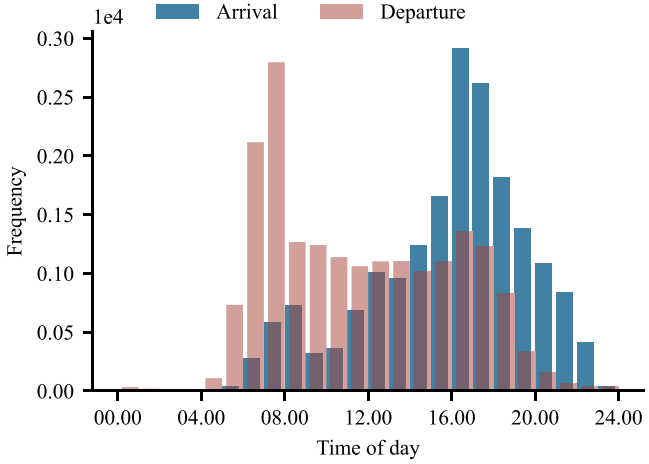


**Fig. 5.** Average hourly arrival and departure counts. Two peaks correspond to charging sessions at home and work. Based on the data generated from the model in [64].

$k$th row to the right by $k - 1$ elements and patching $K - 1$ zeros at each row. Fig. 4 illustrates the process. The same operation on $\mathbf{E}_d$ results in $\mathbf{e}_a$ and $\mathbf{e}_d$, which denote the newly added energy demand and the additional required energy to fulfill the energy demand for the departing EVs at each time index, respectively.

Based on $\mathbf{n}_a$ and $\mathbf{n}_d$, which denote the number of arrivals and departures over the year, Fig. 5 shows the average hourly arrival and departure frequencies. As seen, two peaks in the arrival and departure correspond to charging sessions at home and work: 80% of the charging sessions will arrive in the evening and depart the following day in the morning, i.e., charge at home, and the other 20% will arrive in the morning and depart in the evening, i.e., charge at work. Similarly, based on $\mathbf{e}_a$, which denotes the energy demand for the arriving EVs over the year, Fig. 6 shows the average hourly aggregated energy demand for the arriving EVs and their aggregated stored energy, and the summation gives the average aggregated battery capacity. The energy demand is

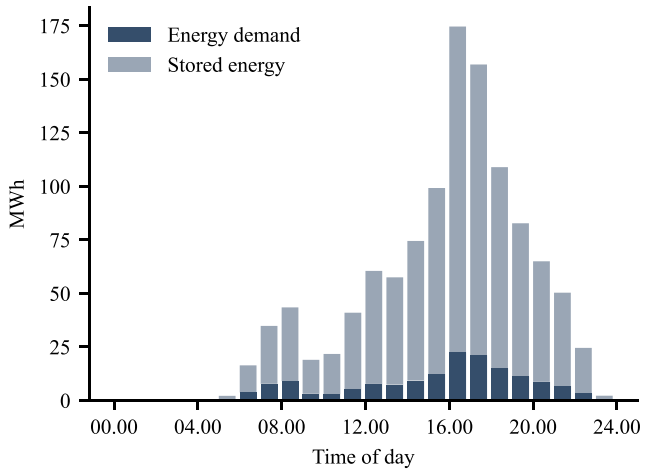


**Fig. 6.** Average hourly aggregated energy demand for the arriving EVs and their aggregated stored energy. Based on the data generated from the model in [64].

relatively small compared to the battery capacity, meaning the required charging time is short. Combined with the long stay duration at home and work, the charging behavior has considerable flexibility to be explored by different smart charging strategies.

### 2.3. Optimization formulation for smart charging and V2G aggregated dispatch

This section presents the mathematical formulation for smart charging and smart charging with V2G for aggregated EVs. This work aims to assess the energy system performance potential with historical data, which is the foundation for future real-time energy system optimization. Thus, the approach shall be valid for both cases. Given uncertainties in real-time implementations, feedback controls such as receding horizon control or model predictive control are often chosen [71]. This work will apply receding horizon control (RHC) with a moving scheduling horizon of 24 h, which reduces the computational complexity compared to scheduling for the whole horizon [72]. Besides, aiming to find the global optimum over the entire year may fail due to the increased number of decision variables and constraints (thus increased computational complexity). However, to provide a comparison and better understanding, this work starts with offline formulation where all the information is available and later points out the required adaption to achieve RHC. The RHC only assumes awareness of the information for the arrived EVs.

The objective is to minimize the mismatch between produced and consumed power. Minimizing the mismatch between produced and consumed power is a common optimization objective in renewable-based energy systems which leads to both improved load matching and reduced peak loads [35,46]. The produced power consists of the RES production $\mathbf{p}_{\text{RES}}$ and the potential vehicle-to-grid discharging (0 in the smart charging case), while the consumed power consists of the base load $\mathbf{p}_{\text{L}}$, the fixed grid-to-vehicle charging $\mathbf{p}_{\text{fix}}$, and the smart charging:

$$\mathbf{p}_{\text{prod}} = \mathbf{p}_{\text{RES}} - \min\left(\mathbf{0}, \mathbf{p}_{\text{agg}}\right), \tag{1}$$

$$\mathbf{p}_{\text{cons}} = \mathbf{p}_{\text{L}} + \mathbf{p}_{\text{fix}} + \max\left(\mathbf{0}, \mathbf{p}_{\text{agg}}\right), \tag{2}$$

where $\mathbf{p}_{\text{agg}} \in \mathbb{R}^{K\times 1}$ denotes the aggregated charging/discharging power, with the positive values meaning charging and the negative values meaning discharging. The mismatch minimization can be formulated as a least-square problem:

$$\min_{\mathbf{p}_{\text{agg}}} \quad \left\|\mathbf{p}_{\text{prod}} - \mathbf{p}_{\text{cons}}\right\|^2. \tag{3}$$

Let $\mathbf{c}_{\text{p}} \in \mathbb{R}_{\geq 0}^{K\times 1}$ and $\mathbf{c}_{\text{e}} \in \mathbb{R}_{\geq 0}^{K\times 1}$ denote the number of connected EVs during and at the end of each time slot, respectively. They can be acquired by:

$$\mathbf{c}_{\text{p}} = \mathbf{A}\left(\mathbf{n}_{\text{a}} - \mathbf{n}_{\text{d}}\right) + \mathbf{n}_{\text{d}}, \tag{4}$$

$$\mathbf{c}_{\text{e}} = \mathbf{A}\left(\mathbf{n}_{\text{a}} - \mathbf{n}_{\text{d}}\right), \tag{5}$$

where $\mathbf{A}$ is an auxiliary matrix where the lower triangular part is 1 while the rest elements are zeros. The purpose of matrix multiplication with $\mathbf{A}$ is to get the cumulative sum.

The aggregated charging power $\mathbf{p}_{\text{agg}}$ depends on the number of connected EVs during each time slot, i.e., $\mathbf{c}_{\text{p}}$. As mentioned, $\mathbf{e}_{\text{a}}$ is the newly added energy demand at each time index. Consequently, $\left(E_{\text{EV,max}}\mathbf{n}_{\text{a}} - \mathbf{e}_{\text{a}}\right)$ denotes the newly added stored energy from the arriving EVs. The aggregated energy balance at the end of each time slot, denoted by $\mathbf{e}_{\text{agg}}$, is constrained by $\mathbf{c}_{\text{e}}$, and it consists of:

- The energy balance by the end of the previous step, denoted as "initial";
- The added energy from the newly arrived EVs, denoted as "arrival";
- The removed energy from the newly departed EVs (must be fully charged), denoted as "departure";
- The added/removed energy from the charging/discharging activity, denoted as "variable".

Thus, the aggregated energy balance at the end of time slot $k$ is:

$$[e_{\text{agg}}]_k = \underbrace{[e_{\text{agg}}]_{k-1}}_{\text{"initial"}} + \underbrace{E_{\text{EV,max}}[n_{\text{a}}]_k - [e_{\text{a}}]_k}_{\text{"arrival"}} - \underbrace{E_{\text{EV,max}}[n_{\text{d}}]_k}_{\text{"departure"}} + \underbrace{\tau[p_{\text{agg}}]_k}_{\text{"variable"}}, \tag{6}$$

where $E_{\text{EV,max}}$ is both the maximum energy for an EV battery and the required energy in the battery for a departing EV. The above equation can be reformulated in vector form (similar to Eq. (11) in [55]):

$$\mathbf{e}_{\text{agg}} = e_{\text{init}}\mathbf{1}_{K\times 1} + \mathbf{A}\left(E_{\text{EV,max}}\mathbf{n}_{\text{a}} - \mathbf{e}_{\text{a}}\right) - E_{\text{EV,max}}\mathbf{A}\mathbf{n}_{\text{d}} + \tau\mathbf{A}\mathbf{p}_{\text{agg}}, \tag{7}$$

where $e_{\text{init}}$ denotes $[e_{\text{agg}}]_0$, and it is 0 if the considered number of arrived EVs before the scheduling horizon is 0. The purpose of using the vector $\mathbf{1}_{K\times 1}$ is to extend the scale variable $e_{\text{init}}$ to the shape $K \times 1$ so that the shape from each part of the right-hand side matches.

Fig. 7, as an example, illustrates how the individual EV affects the aggregated energy balance. During time step 1, there are arrival and charging activities; in time step 2, there are departure and discharging activity; in time step 3, there are arrival, departure, and discharging activity; in time step 4, there are only charging activities; and during time step 5, there are only departures. Accordingly, the aggregated energy balance must consider the corresponding activities by the end of each time step.

#### 2.3.1. Smart charging

In smart charging, $\mathbf{c}_{\text{p}}$ limits the aggregated charging power, and $\mathbf{c}_{\text{e}}$ limits the stored energy in the aggregated EVs. Additionally, to avoid undesirable vehicle-to-vehicle charging, the grid must at least have delivered energy to cover the energy demand of those departing EVs, which is $\mathbf{e}_{\text{d}}$. Consequently, smart charging is formulated as:

$$\mathbf{p}_{\text{sc}} = \arg\min_{\mathbf{p}_{\text{agg}}} \quad \left\|\mathbf{p}_{\text{prod}} - \mathbf{p}_{\text{cons}}\right\|^2,$$
$$\text{s.t.} \begin{cases} \mathbf{0} \preceq \mathbf{p}_{\text{agg}} \preceq P_{\text{EV,max}}\mathbf{c}_{\text{p}}, \\ E_{\text{EV,min}}\mathbf{c}_{\text{e}} \preceq \mathbf{e}_{\text{agg}} \preceq E_{\text{EV,max}}\mathbf{c}_{\text{e}}, \\ \mathbf{A}\mathbf{e}_{\text{d}} \preceq \tau\mathbf{A}\mathbf{p}_{\text{agg}}, \end{cases} \tag{8}$$

where the aggregated charging power at each time index should follow the first constraint, the second constraint is to limit the aggregated stored energy, and the last constraint is to ensure that the minimum energy the grid must have delivered should cover the required energy

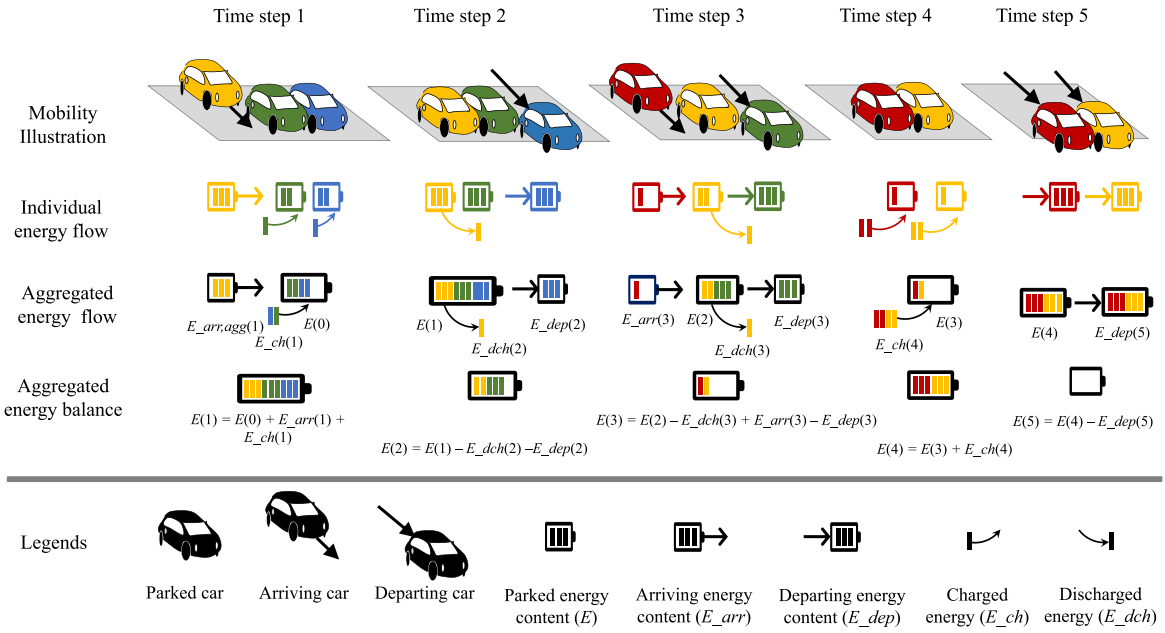


**Fig. 7.** Illustration of EV mobility, individual and aggregated stored energy to visualize the intermittent energy storage concept. By the end of each time slot, the stored energy incipiently consists of 4 items, as in Eq. (6). Practically, it varies, as shown in the row "Aggregated energy balance". Note that, $E_{\text{arr}}(k)$ denotes the arrived energy at the beginning of $k$, $E(k)$ and $E_{\text{dep}}(k)$ denotes the stored energy and the departing energy by the end of $k$, $E_{\text{ch}}(k)$ and $E_{\text{dch}}(k)$ denote the charged and discharged energy during $k$.

to fulfill the energy demand for the departing EVs. This extra constraint aims to prevent undesirable vehicle-to-vehicle charging, which avoids overestimating the performance of smart charging without V2G [55].

### 2.3.2. Smart charging with V2G

The EVs can discharge with the V2G scheme, but the stored energy should stay above the minimum. Thus, smart charging with V2G is formulated as [55]:

$$\begin{aligned} \mathbf{p}_{\text{v2g}} &= \arg\min_{\mathbf{p}_{\text{agg}}} \quad \left\| \mathbf{p}_{\text{prod}} - \mathbf{p}_{\text{cons}} \right\|^2, \\ \text{s.t.} &\begin{cases} -P_{\text{EV,max}}\mathbf{c}_{\text{p}} \preceq \mathbf{p}_{\text{agg}} \preceq P_{\text{EV,max}}\mathbf{c}_{\text{p}}, \\ E_{\text{EV,min}}\mathbf{c}_{\text{e}} \preceq \mathbf{e}_{\text{agg}} \preceq E_{\text{EV,max}}\mathbf{c}_{\text{e}}, \end{cases} \end{aligned} \tag{9}$$

where $E_{\text{EV,min}}$ is the minimum stored energy for an EV. Compared to the smart charging formulation in Eq. (8), the negative lower bound on the charging power denotes the discharging capability.

### 2.3.3. Receding horizon control

The offline formulation aids in comprehending the modeling of the scheduling problem. However, solving a problem that spans the whole year can take a long time due to the number of decision variables and the constraints. RHC, at each time index $k \in \{1, \dots, K\}$, aims to find the best solution for the next $D$ (96 in this study, i.e., 24 h) time slots. Correspondingly, the dimensions of the vectors and matrices should be changed accordingly. Table 2 shows the parameter comparison between the offline control and the RHC. Note that, it requires new parameters to implement RHC compared to the offline control.

In Table 2, $n_{\text{a},k}$ denotes how many EVs arrive at the time index $k$ (the future arrivals are unknown), and it is exactly the $k$th element of $\mathbf{n}_{\text{a}}$. $\mathbf{n}_{\text{D},k}$ is a temporary vector that can capture the departing time index that is out of the scheduling horizon $D$, i.e., when the EV's maximum stay duration is more than 24 h (unnecessary if $D \geq M$). Then, $\mathbf{n}_{\text{d},k}$ is the first $D$ elements from $\mathbf{n}_{\text{D},k}$. $\mathbf{n}_{\text{D},k}$ stores the departure information for the arrived (including time index $k$) yet not departed EVs:

$$\mathbf{n}_{\text{D},k} = \underbrace{\left([T_{\text{d}}]_{k,:}\right)^{\text{T}}}_{\text{newly arrived EVs at } k} + \underbrace{\text{shf}(\mathbf{n}_{\text{D},k-1})}_{\text{EVs arrived before } k \text{ and still are connected at } k}, \tag{10}$$

where "$k, :$" indicates the $k$th row vector, and shf$(\cdot)$ is the shift operation to shift the vector to the lower side by one element, i.e., shf$(\mathbf{n}_{\text{D},k-1})$ results in a new vector $\left[[n_{\text{D},k-1}]_2, \dots, [n_{\text{D},k-1}]_M, 0\right]^{\text{T}}$. Let $n_{\text{A},k}$ denote how many EVs have arrived before (including) the time index $k$. Similar to $\mathbf{n}_{\text{D},k}$, it also has two parts (newly arrival at $k$ and those arrived before $k$ and are still connected):

$$n_{\text{A},k} = n_{\text{a},k} + \sum_{i=2}^{M} [n_{\text{D},k-1}]_i. \tag{11}$$

Similar to the offline control, $\mathbf{c}_{\text{p},k}$ and $\mathbf{c}_{\text{e},k}$ denote the number of connected EVs during and at the end of each time slot within the new scheduling horizon, respectively. They can be acquired by:

$$\mathbf{c}_{\text{p},k} = n_{\text{A},k}\mathbf{1}_{D\times 1} - \mathbf{A}_k\mathbf{n}_{\text{d},k} + \mathbf{n}_{\text{d},k}, \tag{12}$$

$$\mathbf{c}_{\text{e},k} = n_{\text{A},k}\mathbf{1}_{D\times 1} - \mathbf{A}_k\mathbf{n}_{\text{d},k}, \tag{13}$$

where the purpose of $\mathbf{1}_{D\times 1}$ is to extend the scale variable to a vector to match the shape at the right-hand side. $\mathbf{c}_{\text{p},k}$ will be a useful coefficient

**Table 2**
Parameter comparison between the offline control and the RHC.

| Offline | | RHC | |
|---|---|---|---|
| Parameter | Dimension | Parameter | Dimension |
| $\mathbf{n}_{\text{a}}$ | $K$ | $n_{\text{a},k}$ | 1 |
| $\mathbf{n}_{\text{d}}$ | $K$ | $\mathbf{n}_{\text{d},k}$ | D |
| – | – | $n_{\text{A},k}$ | 1 |
| – | – | $\mathbf{n}_{\text{D},k}$ | M |
| $\mathbf{c}_{\text{p}}$ | $K$ | $\mathbf{c}_{\text{p},k}$ | $D$ |
| $\mathbf{c}_{\text{e}}$ | $K$ | $\mathbf{c}_{\text{e},k}$ | $D$ |
| $\mathbf{e}_{\text{a}}$ | $K$ | $e_{\text{a},k}$ | 1 |
| $\mathbf{e}_{\text{d}}$ | $K$ | $\mathbf{e}_{\text{d},k}$ | D |
| – | – | $\mathbf{e}_{\text{D},k}$ | M |
| $e_{\text{init}}$ | 1 | $e_{\text{init},k}$ | 1 |
| – | – | $e_{\text{charged},k}$ | 1 |
| – | – | $e_{\text{lb},k}$ | 1 |
| $\mathbf{A}$ | $K \times K$ | $\mathbf{A}_k$ | $D \times D$ |

to constrain the aggregated charging power while $\mathbf{c}_{e,k}$ is to constrain the aggregated stored energy.

Similarly, $e_{a,k}$, $\mathbf{e}_{D,k}$, and $\mathbf{e}_{d,k}$ are acquired in the same way as $n_{a,k}$, $\mathbf{n}_{D,k}$, and $\mathbf{n}_{d,k}$, where $e_{a,k}$ denotes the aggregated stored energy from the newly arriving EVs at $k$ and $\mathbf{e}_{D,k}$ denotes aggregated energy demand at different departure time index.

Compared to $e_{\text{init}}$, $e_{\text{init},k}$ denotes the stored energy by the end of the time index $k-1$, which consists of the initial stored energy, added stored energy (battery capacity minus energy demand) from the newly arriving EVs, removed stored energy due to the departing EVs, and charged/discharged energy from the connected EVs at time index $k-1$ (similar to Eq. (6)):

$$e_{\text{init},k} = e_{\text{init},k-1} + E_{\text{EV,max}} n_{a,k-1} - e_{a,k-1} - E_{\text{EV,max}}[n_{d,k-1}]_1 + \tau[p^*_{\text{agg},k-1}]_1, \tag{14}$$

where $[p^*_{\text{agg},k-1}]_1$ indicates that $e_{\text{init},k}$ is updated by applying the first time slot of the best (optimal) solution from the time slot $k-1$, which is $\mathbf{p}^*_{\text{agg},k-1}$. Then, the aggregated energy for the scheduling horizon at time index $k$ is:

$$\mathbf{e}_{\text{agg},k} = e_{\text{init},k}\mathbf{1}_{D\times 1} + \left(E_{\text{EV,max}} n_{a,k} - e_{a,k}\right)\mathbf{1}_{D\times 1} - E_{\text{EV,max}}\mathbf{A}\mathbf{n}_{d,k} + \tau\mathbf{A}\mathbf{p}_{\text{agg},k}. \tag{15}$$

The two new parameters in Table 2, $e_{\text{charged},k}$ and $e_{\text{lb},k}$, are necessary to address the constraint for the smart charging,

$$e_{\text{charged},k} = e_{\text{charged},k-1} + \tau[p^*_{\text{agg},k-1}]_1, \tag{16}$$

$$e_{\text{lb},k} = e_{\text{lb},k-1} + [e_{d,k-1}]_1, \tag{17}$$

where $e_{\text{charged},k}$ records how much energy has been provided to EVs before time index $k$, and $e_{\text{lb},k}$ denotes the total energy demand from the EVs that have departed before time index $k$.

Consequently, the smart charging optimization formulation at each time index $k$ is (similar to Eq. (8)):

$$\mathbf{p}_{\text{sc},k} = \arg\min_{\mathbf{p}_{\text{agg},k}} \left\|\mathbf{p}_{\text{prod}} - \mathbf{p}_{\text{cons}}\right\|^2,$$
$$\text{s.t.} \begin{cases} \mathbf{0} \preceq \mathbf{p}_{\text{agg},k} \preceq P_{\text{EV,max}}\mathbf{c}_{p,k}, \\ \mathbf{e}_{\text{agg},k} \preceq E_{\text{EV,max}}\mathbf{c}_{e,k}, \\ e_{\text{lb},k}\mathbf{1}_{D\times 1} + \mathbf{A}_k\mathbf{e}_{d,k} \preceq e_{\text{charged},k}\mathbf{1}_{D\times 1} + \tau\mathbf{A}_k\mathbf{p}_{\text{agg},k}, \end{cases} \tag{18}$$

while the formulation for smart charging with V2G is (similar to Eq. (9)):

$$\mathbf{p}_{\text{v2g},k} = \arg\min_{\mathbf{p}_{\text{agg},k}} \left\|\mathbf{p}_{\text{prod}} - \mathbf{p}_{\text{cons}}\right\|^2,$$
$$\text{s.t.} \begin{cases} -P_{\text{EV,max}}\mathbf{c}_{p,k} \preceq \mathbf{p}_{\text{agg},k} \preceq P_{\text{EV,max}}\mathbf{c}_{p,k}, \\ E_{\text{EV,min}}\mathbf{c}_{e,k} \preceq \mathbf{e}_{\text{agg},k} \preceq E_{\text{EV,max}}\mathbf{c}_{e,k}. \end{cases} \tag{19}$$

### 2.4. Energy matching measures

Four energy matching measures were used to assess the performance of the city-scale energy system:

- Production-to-load ratio (P/L),
- Self-consumption ratio (SC),
- Self-sufficiency ratio (SS),
- Self-consumption-sufficiency balance ratio (SCSB).

The annual production-to-load ratio (P/L) is the fraction of total annual electricity production to the total annual electricity consumption. In a net-zero energy city scenario, P/L should be equal to 1. SC is the fraction of the total self-consumed locally renewable electricity production to the total production. On the other hand, SS is the fraction of the total self-consumed locally renewable electricity production to the total electricity consumption. SCSB conveys the balance between SC and SS.

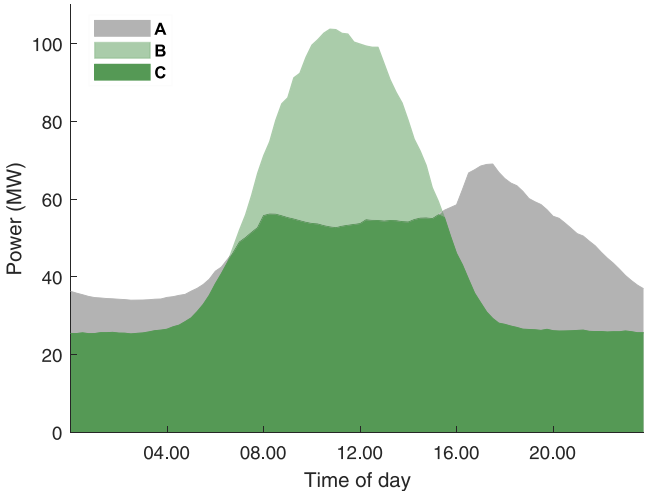


**Fig. 8.** Schematic outline of daily electricity load including EV charging load and renewable generation (wind+PV) profiles. Area **A** represents electricity load including EV charging load not covered by local renewable generation, area **B** represents excess renewable generation not consumed by the city load, and area **C** represents self-consumed renewable electricity within the city. **A**+**C** represents total daily city electricity load and **B**+**C** represents total city renewable electricity generation.

Fig. 8 shows the schematic outline of daily electricity load (including EV charging load), renewable generation, and self-consumed renewable electricity within the city. Even though the assessment is conducted on an annual basis, the daily illustration in Fig. 8 can help to understand these measures, which from the areas in the figure can be defined as

$$\text{P/L} = \frac{\text{A+C}}{\text{B+C}}, \tag{20}$$

$$\text{SC} = \frac{\text{C}}{\text{B+C}}, \tag{21}$$

$$\text{SS} = \frac{\text{C}}{\text{A+C}}. \tag{22}$$

Mathematically, the self-consumed power at time $t$, can be defined as

$$m_t = \min(p_{\text{prod},t}, p_{\text{cons},t}), \tag{23}$$

And P/L, SC, and SS can be defined mathematically as [33]

$$\phi_{P/L} = \frac{\int p_{\text{prod},t}\,dt}{\int p_{\text{cons},t}\,dt}, \tag{24}$$

$$\phi_{SC} = \frac{\int m_t\,dt}{\int p_{\text{prod},t}\,dt}, \tag{25}$$

$$\phi_{SS} = \frac{\int m_t\,dt}{\int p_{\text{cons},t}\,dt}. \tag{26}$$

Interested readers are referred to [25] for more detailed relation between P/L, SC, and SS.

Since SC tends to be lower when generation is high, while the opposite happens for SS, there should be a measure that conveys the balance between the two. SCSB is the measure that conveys the balance between SC and SS. With this measure, the optimal trade-off between SC and SS can be defined. Using the harmonic mean of SC and SS, SCSB can be defined mathematically as [21]:

$$\phi_{SCSB} = \frac{2\phi_{SC}\phi_{SS}}{\phi_{SC} + \phi_{SS}}. \tag{27}$$

Since both SC and SS range between 0 and 1, the SCSB score also ranges from 0 to 1. Based on Eq. (27), a high SCSB score can only be

achieved if both SC and SS are high. If the generation unit is undersized compared to the load, SC tends to be high since most of the local generation is self-consumed, but SS tends to be low since a significant amount of the demand is not covered by the local load. This results in a low SCSB score since only SC is high but not SS. The SCSB will still be low if the generation unit is oversized compared to the load since, in that case, SS tends to be high due to most load being covered by local generation, but SC tends to be low since the excess generation is high. To sum up, the SCSB can be used to define the optimal trade-off between SC and SS. Interested readers are referred to [21] for more detailed explanations and applications of the SCSB score. The SCSB score in this paper is used to define the optimal P/L and justify whether a net-zero energy city scenario is an optimal scenario or not.

### 2.5. Simulation scenarios

In order to fulfill the aims of the papers, several scenarios are simulated. Based on the simulation parameters, the simulation scenarios grouping can be divided into four:

- EV charging dispatch scenarios,
- Wind-PV electricity production share scenarios,
- RES-load ratio (P/L) scenarios,
- Stationary energy storage capacity scenarios.

The following subsections present the details on each scenario group.

#### 2.5.1. EV charging dispatch scenarios

There are three aggregated EV charging scenarios: opportunistic charging, smart charging, and V2G. In opportunistic charging, it is assumed that all the EVs start charging upon arrival at the destined charging location. In smart charging scenarios, it is assumed that aggregatedly, the EV charging network can delay its power-consuming activity to match the local generation and avoid the existing peak load. In the V2G scenarios, not only can the aggregated EV charging network optimize its power consumption to achieve a flatter net load, but it can also dispatch power from the aggregated EV battery to the city grid to make the net load even flatter. All mathematical modeling for these three charging scenarios were previously presented in Sections 2.2 and 2.3. The three charging scenarios were simulated in all simulations in this study.

#### 2.5.2. Wind-PV electricity production share scenarios

Different scenarios on wind-PV electricity production share were simulated to find the optimal wind-PV share that maximizes the load matching measures. In the varying wind-PV share simulations, the set-up was a net-zero energy city, which means the P/L was equal to one. It should be noted that, in a net-zero energy city, SC will be equal to SS, which consequently makes the SCSB equal to both as well. Ten shares of wind-PV electricity production on the percentage scale were simulated, starting from 0:100 (wind-PV) with a step of 10:-10 and ending at 100:0.

It should be noted that the wind-PV ratio for electricity production (MWh/MWh) differs from the ratio for nameplate power capacity ($MW_p/MW_p$). However, these ratios are interrelated through the power plant capacity factor (CF) [73]. The relationship between annual electricity production, rated power, and the CF of a power plant can be defined as [73]:

$$E_{\text{plant,annual}} = CF_{\text{plant}} \times P_{\text{plant,rated}} \times 365 \times 24 \text{ h}, \tag{28}$$

where $E_{\text{plant,annual}}$ is the annual electricity production of a power plant (MWh), $CF_{\text{plant}}$ is the CF of a power plant (p.u.), and $P_{\text{plant,rated}}$ is the nameplate rated power capacities of a power plant (MW). Following Eq. (28), the relationship between the wind-PV electricity production ratio and its rated power capacity ratio can be defined as

$$\frac{P_{\text{wind,rated}}}{P_{\text{PV,rated}}} = \frac{E_{\text{wind,annual}}}{E_{\text{PV,annual}}} \times \frac{CF_{\text{PV}}}{CF_{\text{wind}}}, \tag{29}$$

where $P_{\text{wind,rated}}$ and $P_{\text{PV,rated}}$ are the nameplate rated power capacity ($MW_p$), $E_{\text{wind,annual}}$ and $E_{\text{PV,annual}}$ are the annual electricity production, and $CF_{\text{wind}}$ and $CF_{\text{PV}}$ are the CFs of wind and PV power plants, respectively. It is important to note that the validity of Eq. (29) depends on the assumption that all the variables are greater than zero.

Empirical data from wind and solar plants show that their CFs are 0.35 and 0.14, respectively [57]. As an example, suppose the wind-PV electricity production ratio is 70:30 and the rated power of the wind turbine is 70 MW. In this scenario, the rated power of the solar plant would be 75 MW. Notably, even though the wind plant produces more than twice the amount of electricity as the solar plant, the two plants have nearly equal rated power capacities.

#### 2.5.3. RES-load ratio scenarios

After finding the optimal wind-PV electricity production ratio, different scenarios on RES-load ratios, which were previously referred to as P/L ratios, were simulated to find out if the net-zero energy scenario is the optimal set-up in terms of load matching. P/L from 0.80 with a step of 0.05 to 1.20 were simulated. The optimal wind-PV electricity production ratio was set as the generation share in the varying P/L simulation.

#### 2.5.4. Stationary energy storage capacity scenarios

Several scenarios with different capacities of stationary energy storage were simulated. The simulations involving stationary energy storage were conducted to investigate two aspects. The first one is to find out how much stationary energy storage is needed to match the performance of V2G in a net-zero energy city initially without stationary storage. The second one is to find out how big stationary energy storage capacity is needed to make the net-zero energy city self-sufficient (not importing energy from the grid outside of the city). The optimal wind-PV electricity production ratio was set as the generation share in the varying stationary storage simulation.

A simple storage model was used in this paper. The storage is assumed to be charged whenever there is an excess renewable yield that is not consumed by the load. On the other hand, the storage supplies the load when renewable power production is not sufficient to supply the load. Renewable production excess is sent to the transmission grid outside the city if the storage has already reached its maximum energy content. If the storage is low-charged, the transmission grid outside of the city will as usual cover the power deficit. The minimum and maximum energy contents of the storage were set to 0 and the simulated storage capacities, respectively. The C-rate of the storage was set to 1 C, as assumed in several studies on grid storage [74,75]. The charging and discharging efficiency was assumed to be 1. In the real-world setup, important parameters such as efficiency and state-of-charge operating range would not be as ideal as in this simple storage model. However, since the assessment in this paper is to find out the theoretical rather than the practical storage capacity, the simple model is sufficient. Simplistic storage models were previously used in several studies that focused on renewable-based energy systems, such as in [42,76,77].

## 3. Results

This section presents the results on the impacts of opportunistic charging, smart charging, and V2G in urban-scale energy matching. Specifically, Section 3.1 provides results on optimal wind-PV electricity production ratio in achieving optimal load matching in the net-zero energy city. Section 3.2 presents the optimal RES-load ratio assessment. The performance in the optimal net-zero energy city is presented in Section 3.3. Assessments on the value of V2G compared to stationary storage, as well as the stationary storage required to achieve a self-sufficient city, are provided in Section 3.4.

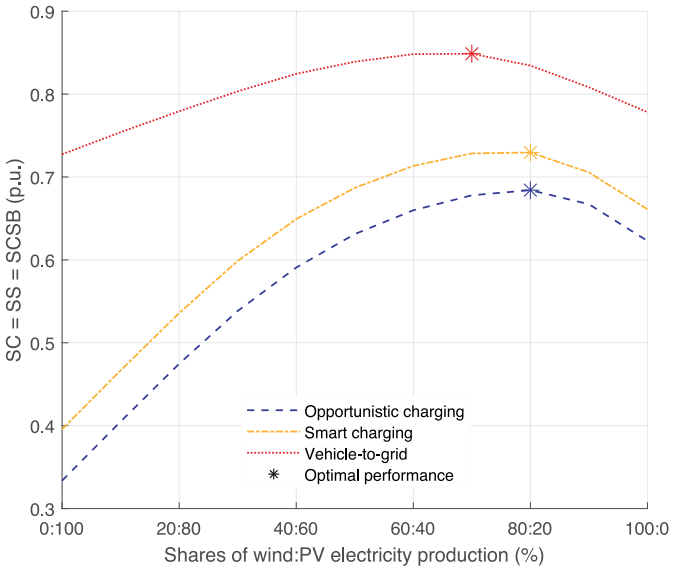


**Fig. 9.** City load matching performance with three different EV charging scenarios and different shares of wind-PV. Starred points indicate the optimal wind-PV shares in the respective charging scenarios.

### 3.1. Optimal wind-PV electricity production shares in a net-zero energy city

Fig. 9 shows the SC, which is equal to SS and SCSB in the case of net-zero energy systems where electricity production equals electricity consumption, against different wind and PV shares scenarios. It can be seen that in all wind-PV scenarios, SCSB scores in the V2G scenarios are higher than the ones in the smart charging scenarios, which are higher than the ones in the opportunistic charging scenarios. From the figure, it is shown that the optimal wind-PV electricity production ratio scenarios are 80:20 for the opportunistic and smart charging scenarios, and 70:30 for the V2G scenarios.

Fig. 9 shows that the 100% PV scenario has the lowest SCSB values among the simulated wind-PV electricity production share scenarios. In the 100% PV scenario, it can also be seen that the differences in the SCSB scores between V2G and the other two charging scenarios are the highest. That implies the higher importance of V2G in a 100% PV-powered net-zero energy city, compared to the other wind-PV scenarios. This can be explained by seasonal patterns of electricity production and load.

Fig. 10(a)–(d) show the 30-day moving mean power production and load in 50:50, 100:0, 0:100, and 70:30 (optimal) wind-PV electricity share scenarios. Fig. 10 illustrates the correlation between the production and load on a seasonal basis, which is crucial for assessing the load matching performance. In Fig. 10, the uncontrolled charging profiles were used to generate the 30-day moving mean EV charging profiles. It should be noted that the 30-day moving mean EV charging profiles for uncontrolled charging, smart charging, and V2G scenarios are approximately the same, considering that the flexibilities of EVs are limited to hours, or at most, a few days. In this case, the EV charging demand can only be shifted with smart charging and V2G to different hours, or to the next day, and not to different months.

It can be seen, especially in Fig. 10(c), that the seasonal pattern of PV electricity production is highly anti-correlated with the seasonal pattern of the load. This is due to the fact that during winter, the load is at its highest while the solar production is at its lowest, and vice versa. On the other hand, it can be seen, especially in Fig. 10(b), that the seasonal pattern of wind electricity production is highly correlated with the seasonal pattern of the load.

Despite the high seasonal correlation between wind power production and load, the optimal wind-PV electricity production share is not 100% wind and 0% PV. This is because, besides the seasonal correlation, the diurnal correlation between electricity production and load is also crucial in defining the optimal RES share. The averaged diurnal patterns of electricity production and load are shown in Fig. 11.

From Fig. 11, it can be seen that, the wind power production is slightly higher during the night than during the noon, while the solar power production peaks during the mid-noon and non-existence during the night. The city load is at its lowest at night and peaks during the afternoon–evening. From a diurnal perspective as shown in the figure, an excessive reliance on wind power would lead to uncovered load during the day and surplus generation at night, while an excessive reliance on solar power would result in overgeneration during the day and insufficient coverage of the load at night. Therefore, an optimal solution can be achieved by combining both wind and solar power, which would enhance the performance of load matching.

To sum up, by visual inspection from Figs. 10 and 11, it can be concluded that the seasonal pattern of the load is highly correlated with that of wind power and anti-correlated with that of solar power. On the other hand, the diurnal pattern of the load is slightly anti-correlated with that of wind power and correlated with that of solar power. Thus, the right combination of wind and PV will have a higher ability to match the consumption patterns, since they complement each other both diurnally and seasonally.

Out of all simulated scenarios, the maximum SCSB performance is reached when the wind-PV electricity production share is 70:30 and V2G is deployed. It should be noted that the wind-PV share in this case is in terms of annual electricity production. Based on Eq. (29) presented in Section 2.5, with an empirical CF of 0.35 for wind and 0.14 for PV in the city, the wind-PV ratio of 70:30 in terms of electricity production (MWh), will be equivalent to 14:15 in terms of nameplate power capacity ($MW_p$), which is close to 1:1.

From Fig. 11, vehicle-to-grid row, it can also be seen that the charging and discharging power in the V2G scenarios is highest in the 100% PV scenario. This strengthens the previously mentioned argument that, in order to reach the optimal matching, the V2G is needed to a larger extent in a 100% PV-powered net-zero energy city.

### 3.2. Optimal RES-load ratio in the city

Fig. 12(a)–(c) shows the SC, SS, and SCSB of the renewable-powered city with three different EV charging scenarios in different production-to-load (P/L) ratios. Fig. 12(a) shows that the higher the P/L ratio, the lower the SC, and Fig. 12(b) shows that the higher the P/L ratio, the higher the SS. From Fig. 12(c), it can be seen that the SCSB plots are concave-shaped, which means that there is one optimal P/L value. From the figure, it is shown that the optimal city-scale P/L is 0.85 in the opportunistic and smart charging scenarios, and 1.00 in the V2G scenario.

These results show that without V2G acting as the intermittent storage, the net-zero energy city scenario, where P/L is 1, is not the optimal scenario in terms of trade-offs between self-consumption and self-sufficiency. That means that by increasing the generation scale from 0.85 to 1, the increase in self-sufficiency is lower than the decrease in self-consumption if V2G is not deployed. This is different from the condition where V2G is deployed. With V2G, the net-zero energy city is the optimal scenario where trade-offs between SC and SS peak. These results highlight the important role of V2G schemes or energy storage in general if a high self-sufficiency is to be achieved for a net-zero energy city.

### 3.3. Detailed performance in the optimal net-zero energy city

This section presents more detailed results on the performance of the optimal net-zero energy city, which has a P/L of 1.00 and wind-PV electricity production share of 70:30.

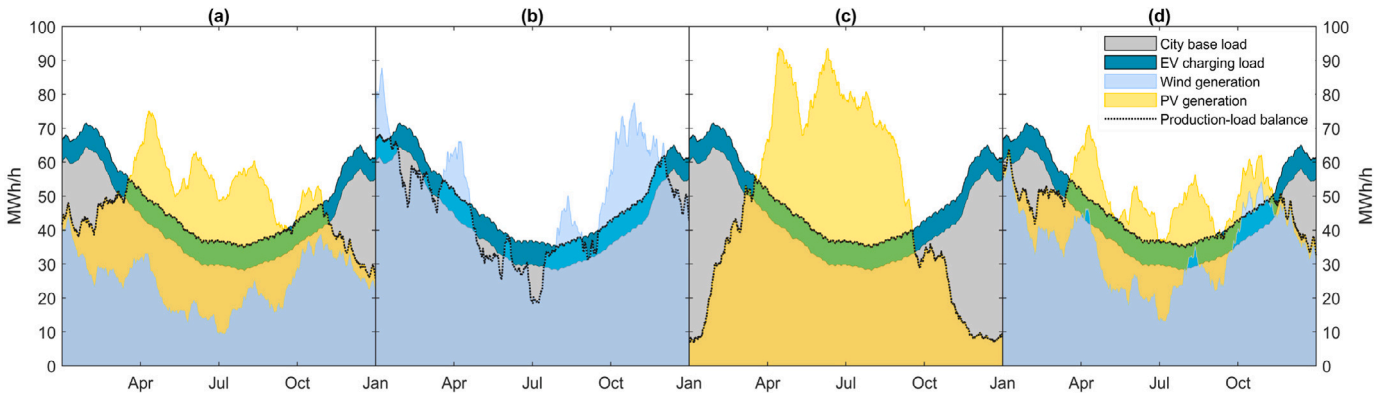


**Fig. 10.** 30-day moving mean electricity production and load in (a) 50% wind : 50% PV, (b) 100% wind, (c) 100% PV and (d) 70% wind : 30% PV (optimal) scenarios. The figure illustrates the seasonal correlation between production and load, and provides an approximation of the seasonal load matching performance at various wind-PV electricity shares.

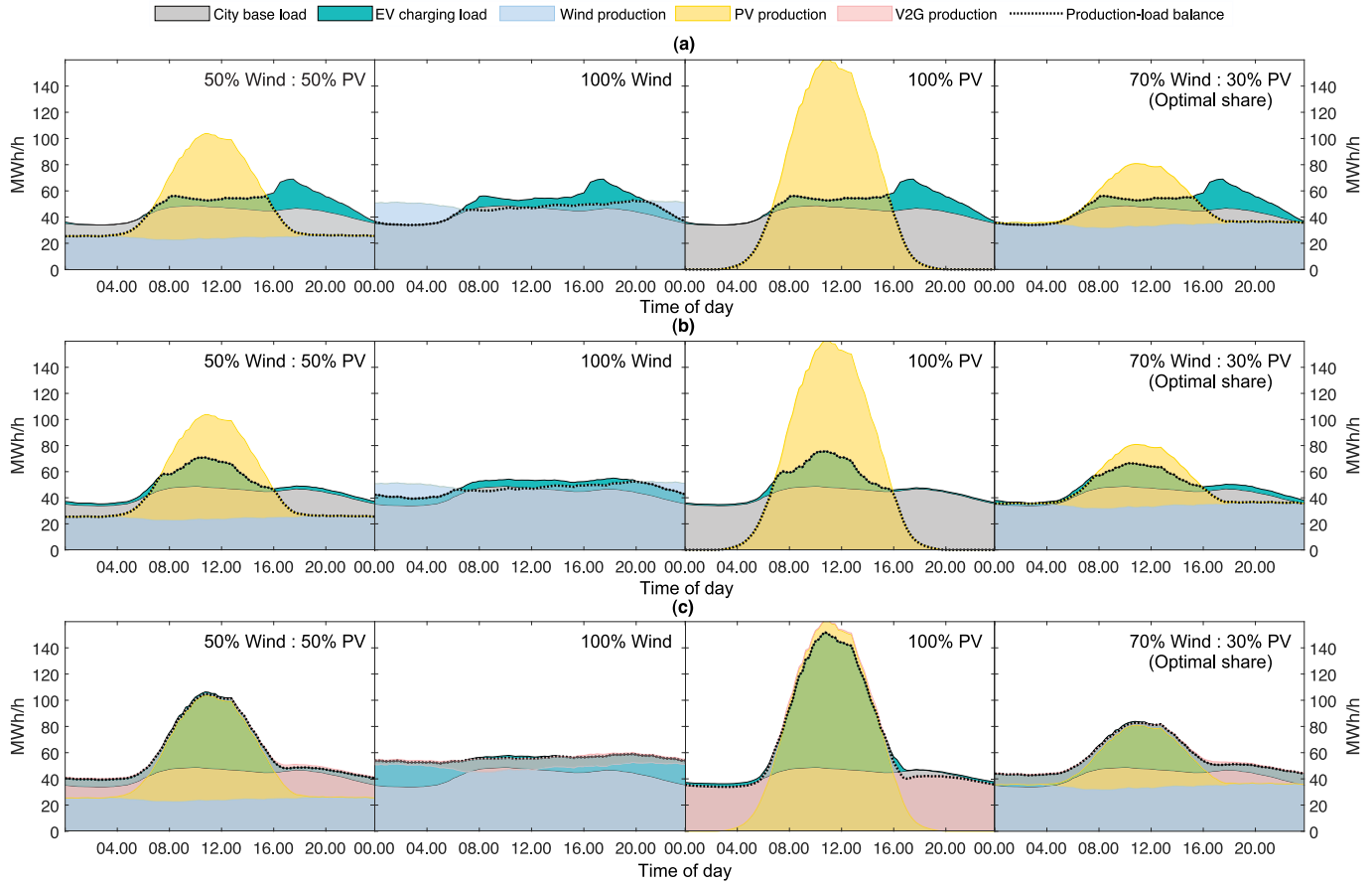


**Fig. 11.** Daily average of power production (transparent areas) and load (solid areas) in (a) uncontrolled charging, (b) smart charging and (c) V2G scenarios for four different wind-PV electricity production shares. The figure illustrates the diurnal correlation between production and load, and provides an approximation of the daily load matching performance at various wind-PV electricity shares.

### *3.3.1. Generation-load profiles*

In this section, the load profiles in different EV charging scenarios are analyzed. The goal is to understand the impact of opportunistic charging, smart charging, and V2G on both peak net load and peak net generation. Peak net load represents the maximum value of load minus generation, while peak net generation or peak excess generation corresponds to the maximum value of generation minus load. As previously mentioned in Section 2.1, the base peak load without local generation is 94 MW. In the net-zero energy city scenario with optimal wind-PV generation share (i.e., 70% wind - 30% PV), the peak load can be reduced to 75 MW. Table 3 shows the annual peak net load and peak net generation in different EV charging scenarios.

As it can be seen in Table 3, the addition of opportunistic charging demand will increase the urban peak net load, from 75 MW to 104 MW. The addition of EV charging demand with smart charging deployment does not increase the peak net load. Furthermore, the integration of urban EV fleets equipped with V2G capability can decrease the peak load from 75 MW to 58 MW.

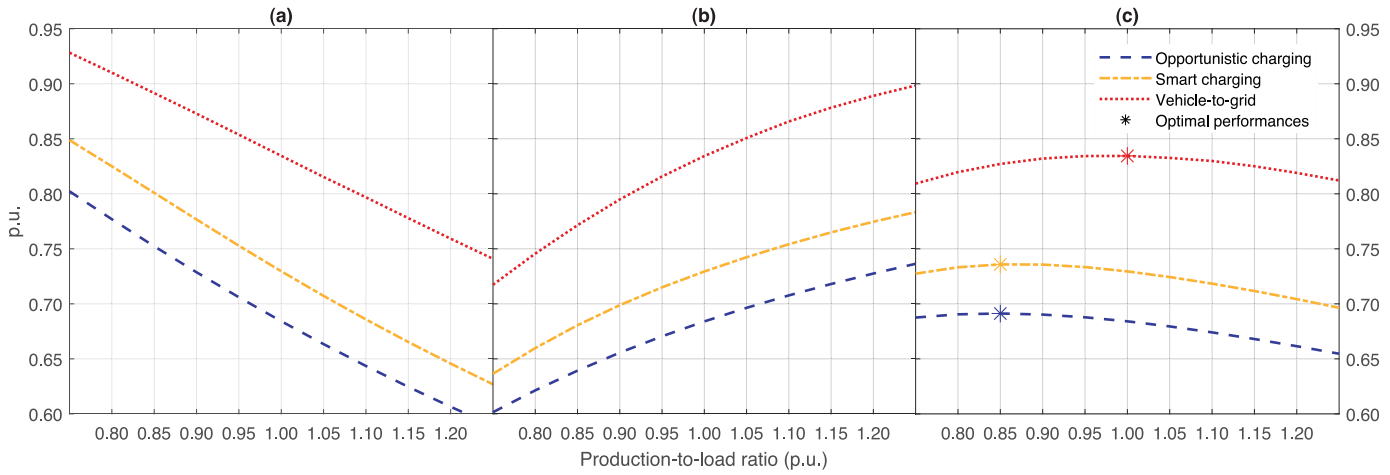


**Fig. 12.** Performance of (a) SC, (b) SS, and (c) SCSB in different P/L ratios and EV charging scenarios. Starred points indicate the optimal RES-load ratios in the respective charging scenarios.

**Table 3**
Peak net-load and peak net-generation in net-zero energy city scenario,.

| Scenario | Peak net load (MW) | Peak net generation (MW) |
|---|---|---|
| No EVs | 75 | 168 |
| Opportunistic charging | 104 | 165 |
| Smart charging | 75 | 129 |
| Vehicle-to-grid | 58 | 69 |

**Table 4**
Energy matching performance of net-zero energy city in opportunistic charging, smart charging, and V2G scenarios. In the net-zero energy scenario, the SC is equal to the SS, hence the SCSB is equal to both the SC and SS.

| Scenario | SCSB |
|---|---|
| Opportunistic charging | 0.68 p.u. |
| Smart charging | 0.73 p.u. |
| Vehicle-to-grid | 0.84 p.u. |

In terms of peak excess or net generation, the opportunistic charging demand decreases the peak net generation slightly from 168 MW to 165 MW. The peak net generation can be decreased further to 129 MW with smart charging deployment. The deployment of V2G can decrease the peak net generation much more significantly to 69 MW.

These results show that, EVs with smart charging capability act as flexible demand, helping to avoid peak load increases and facilitate valley filling. Additionally, EVs with V2G extend their capability further to peak clipping as well. The phenomena can be further explained by analyzing the load profile in an example week as shown in Fig. 12.

Fig. 13 shows (a) net load (load minus generation), (b) net charging power, and (c) aggregated SOC with different charging scenarios in five September days. In net charging profiles, positive values represent net charging, and negative values represent net discharging. In terms of peak load, Fig. 13(a) shows that the peak electricity load is increased with opportunistic charging demand; see Friday and Monday evenings. With smart charging, the base peak load is not increased. With V2G, the base peak load can even be clipped. In terms of excess generation (negative load), Fig. 13(a) shows that the opportunistic charging scheme barely reduces the generation excess, while the smart charging scheme can reduce it to some extent, and the V2G scheme can reduce it to a greater extent.

This can be explained by Fig. 13(b), where the net charging power is shown. It can be seen that the opportunistic charging load peaks at the same time as the peak base load. In the smart charging scenarios, the charging demand can be delayed to an off-peak period so that it does not increase the peak base load. The smart charging load can also be altered to fit the generation pattern to some extent. In the V2G scenarios, the flexibility of EVs is extended from just being flexible demand to include being flexible generation as well. This can be seen in the negative charging power where the base net load is positive. The ability to reduce the excess generation is also increased since there is more room to charge the EV battery after it has been used for V2G, as shown in Fig. 13(c). On a daily average basis, the aggregated SOC of connected EVs in different charging scenarios can be seen in Fig. 14. It should be noted that the SOC shown in Fig. 14 is on the aggregated level with an assumption that each connected EV reaches full-charge conditions just before the departure time. This represents the technical limits of EV flexibility in terms of SOC in different charging scenarios if EV users' charging demand is not compromised.

### 3.3.2. Load matching performance

Table 4 presents the numerical results on annual energy matching measures in the three different charging scenarios. It should be noted that in a net-zero energy city, energy matching measures for each EV charging scenario, i.e., SC, SS, and SCSB, will be equal. Numerical results show that, there is a 5 percentage point increase from opportunistic charging to smart charging, and an 11 percentage point increase from smart charging to V2G in annual load matching performance. That means that there is a 16 percentage point increase from opportunistic charging to V2G.

Fig. 15 shows the daily average of power production and load in different EV charging scenarios (columns) and different months (rows). In the figure, the solid areas represent the load, and the transparent areas represent the generation. The intersection areas approximate the self-consumed generation. Regardless of the EV charging strategies, there is a load matching variability between different periods.

As can be seen in Fig. 15, during January (winter), the load is at its peak. Even though wind electricity production is also at its peak, solar electricity production is at its lowest. Thus, the largest share of the load not covered by the city power generation occurs during January, which results in low SS, but high SC.

During April (spring), there is a lot of excess generation power. This is due to the PV power being at one of its highest production periods, while both the wind power generation and load are at their medium period. This results in high SS, but low SC, especially in the opportunistic and smart charging scenarios. The load matching performance in October (autumn) is similar to the one in April, but the roles of wind and PV are switched, with the wind being in one of its highest production periods, and PV in a medium production period.

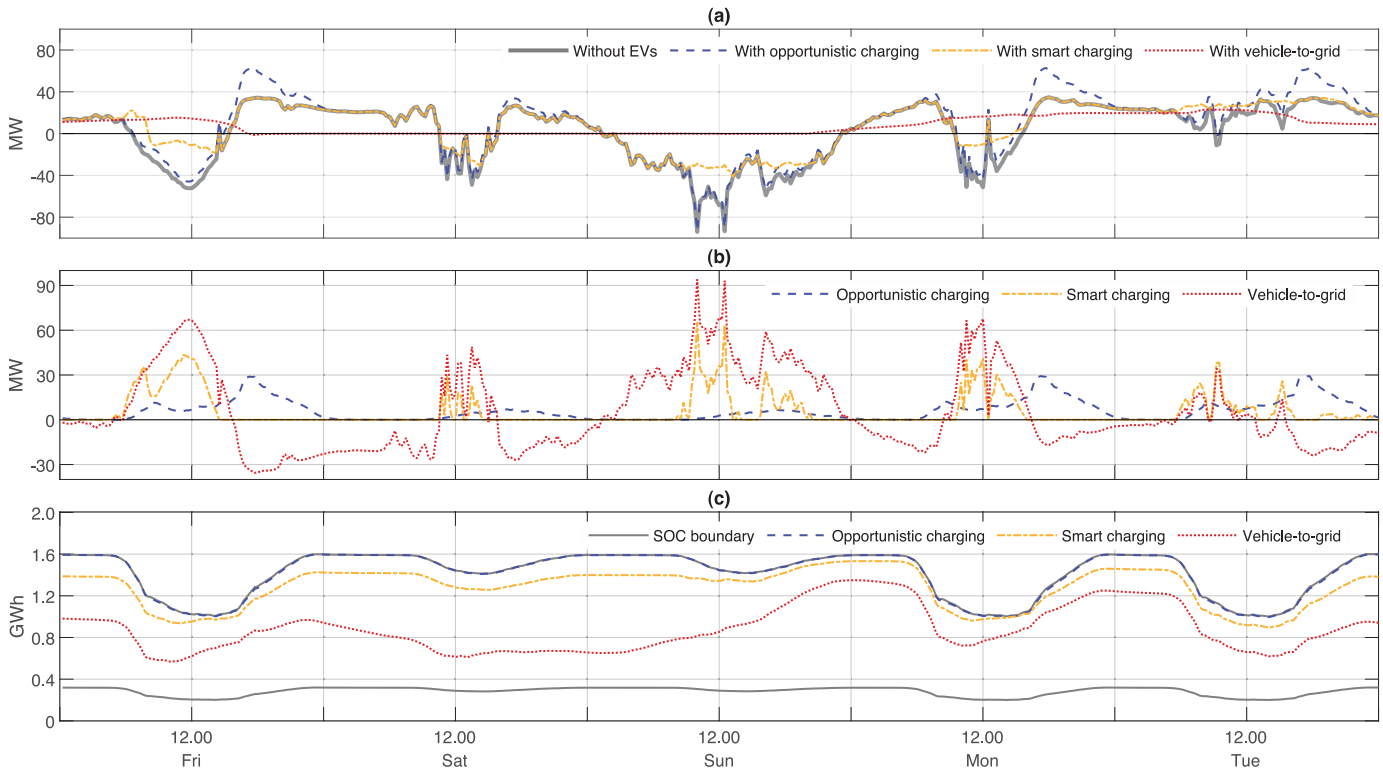


**Fig. 13.** (a) Net load (load minus generation), (b) net charging power (positive values represent charging, and negative values represent discharging) and (c) aggregated SOC of EV batteries connected to the system, with different charging scenarios in five September days.

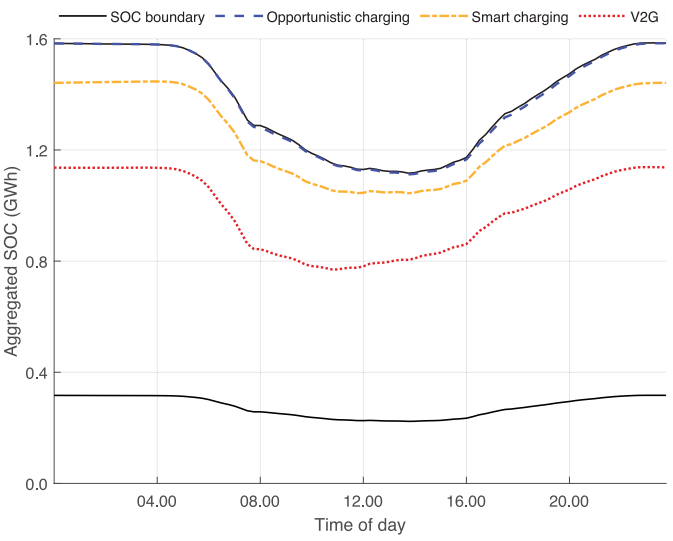


**Fig. 14.** Daily average of aggregated connected EV SOC. The difference between the SOC in the opportunistic charging and V2G scenarios represents the technical limits of the EV flexibility, if the EV users' charging demand is not compromised.

During July (summer), the relatively low energy demand matches the lowest wind, and the high PV power production. This results in high SC, high SS, and consequently high SCSB, especially in the V2G scenarios, where its flexibility is utilized to match the PV production pattern. Fig. 16 shows the 30-day moving mean of daily SC, SS, and SCSB in different EV charging scenarios. It can be seen that the highest SCSB performance is obtained with the V2G scenario between the end of June and the beginning of July.

**Table 5**
Energy storage capacity requirement to reach selected level of self-sufficiency in different EV charging scenarios for the net-zero energy city.

| SS (p.u) | Energy storage capacity required (GWh) | | |
|---|---|---|---|
| | Opportunistic charging | Smart charging | Vehicle-to-grid |
| **0.85** | **1.4** | **1.1** | **0.0** |
| 0.90 | 8.1 | 7.1 | 1.9 |
| 0.95 | 29.8 | 28.6 | 24.1 |
| **1.00** | **51.5** | **50.4** | **49.0** |

### *3.4. The value of V2G and achieving self-sufficient city with stationary energy storage*

This section quantifies the value of the V2G scheme as intermittent energy storage compared to stationary energy storage. This section also provides results on theoretical storage capacities to make the city fully self-sufficient, meaning no imported energy from the transmission/regional grid. It should be noted that with an annual P/L ratio of 1 (net-zero energy city), in order to reach an annual SS of 1 (self-sufficient city) with energy storage, the 1-year simulation should start from a month in which there is high excess energy so that the excess can be stored and used later. If the simulation starts from a month in which the electricity production is less than the consumption, an SS of 1 cannot be reached since the battery is still empty in the beginning and cannot compensate for the uncovered load. For that reason, the simulation started from day 86 to day 365, then continued from day 1 to day 85. With this simulation set-up, the SS without stationary energy storage is insignificantly higher, around 1%, than the ones presented in Section 3.3.2.

Fig. 17 shows the city self-sufficiency with different stationary energy storage capacities for different EV charging scenarios in a net-zero energy city. Table 5 shows the numerical results on how much storage is required to reach SS of 0.85, 0.90, 0.95, and 1.00.

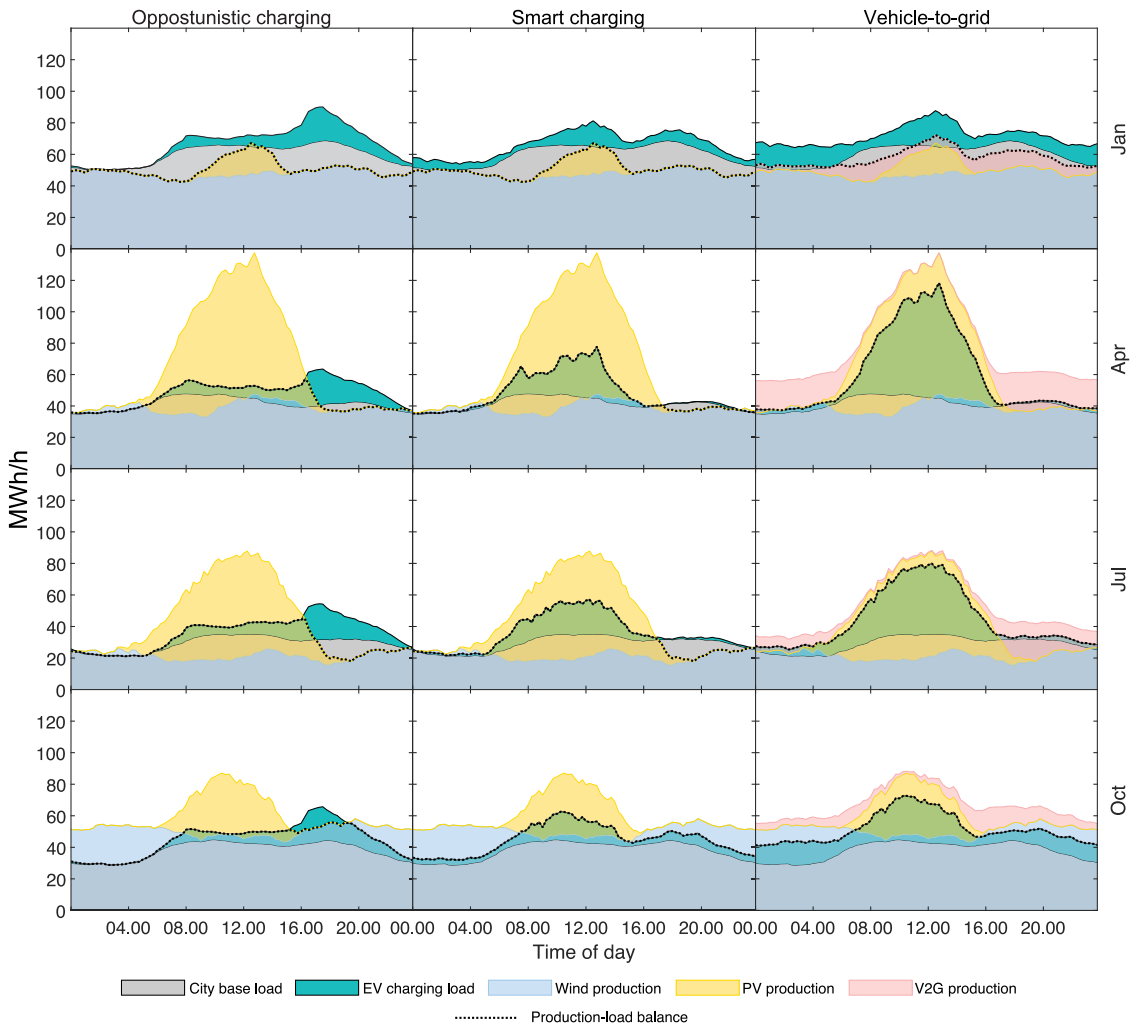


**Fig. 15.** Daily average of power consumption (solid areas) and production (transparent areas) in different EV charging scenarios (columns) and different months (rows). This figure illustrates the load matching with different EV charging scenarios in different seasons within a year.

It should be noted that an SS of 0.85 is reached in the V2G scenario without stationary storage. That implies the energy storage capacities required to reach a SS of 0.85 in the opportunistic and smart charging scenarios correspond to the value of the V2G scheme in the respective scenarios. The results show that the V2G scheme with a 2.4 GWh EV battery involved as intermittent storage, is worth 1.4 and 1.1 GWh stationary energy storage in opportunistic and smart charging scenarios respectively.

In order to reach an SS of 0.90, the opportunistic EV charging, smart EV charging, and V2G scenarios require 8.1, 7.1, and 1.9 GWh respectively. In order to reach an SS of 0.95, all EV charging scenarios require around 21–22 GWh additional storage to the ones required to reach an SS of 0.90. A self-sufficient city, where SS is 1.00, will theoretically be achieved when the storage capacities are 51.5 GWh in the opportunistic EV charging scenario, 50.4 in the smart EV charging scenario, and 49.0 GWh in the V2G scenario, which are around double the sizes required to reach an SS of 0.95. From these results, it can be concluded that it is easier to increase the SS from a low value to a medium value than from a medium value to a high value.

## 4. Discussion

This section discusses and analyzes the main takeaways presented in Section 3 in more detail and further proposes future research related to the findings.

### 4.1. On the EV flexibility utilization in a net-zero energy city

The results in Section 3 show that EV smart charging deployment enhances the city-scale load matching. However, the enhancements are much less significant than the ones achieved with the V2G schemes. EVs are mainly used for transportation. However, a survey found that personal cars, on average, spent 22 h a day being parked, with 16 h of them being uninterrupted parking [78]. With this long parking duration and resulting flexibility, there is vast potential for EV batteries to be exploited as intermittent storage. As long as it does not interfere with its transportation objective, EV flexibility could be utilized by V2G schemes as intermittent storage for power grid balancing purposes.

As mentioned previously in Section 1, the term intermittent energy storage for EV batteries participating in V2G schemes is motivated by the nature of EV batteries not being constantly available and predictable for grid balancing. It is of interest to compare the impact of V2G as intermittent storage to the traditional stationary energy storage on the energy system performance. In Section 3.4, it was estimated that when the EV flexibility with a 2.4 GWh EV battery is fully utilized, the city will achieve a load matching performance similar to the city installing a 1.4 GWh stationary energy storage. It should be noted that this number is the best-case approximation when aggregators know in advance when arriving cars are departing. In reality, the mobility pattern is a stochastic process. The stochastic availability of connected


**Fig. 16.** 30-day moving mean of daily SC, SS, and SCSB in different EV charging scenarios. This figure shows the load matching variability throughout the year.

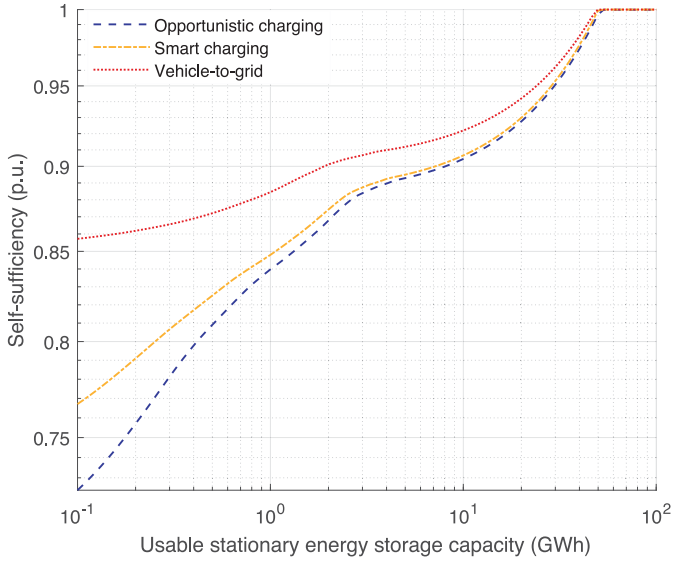


**Fig. 17.** City self-sufficiency with different stationary energy storage capacity in different EV charging scenarios in net-zero energy city.

EV battery capacity needs to be addressed for grid-operation purposes. Studies on probabilistic models of EV availability as energy storage for the power grid are suggested for future research.

The smart charging and V2G approaches in this study have a pure technical objective, i.e., minimizing the mismatch between generation and load. The assessments were conducted to determine the best-case or the highest possible performance that can be achieved with smart charging and V2G schemes on the city-scale. The advantages of technical optimal mainly benefit power grid operators. The technical optimal for the power grid operators and economic optimal for EV aggregators and EV users might be different on many occasions. It is important to note that with V2G schemes, the lifetime of the EV battery could be shortened significantly [79]. EV users might need to replace the battery much earlier than if the EVs were not participating in a V2G scheme. Thus, in a real-world scenario, the V2G scheme participation needs to be compensated by proper economic benefits for EV users.

In future research, it will be interesting to design optimal electricity market models or, in other words, optimal price signal models, so that both technical and economic optimal are reached by users, aggregators, and power grid operators. In this case, the optimal price signal models should also consider the EV battery degradation so that after a number of years, the EV users will have net economic benefits even after replacing their EV battery. This approach will most likely engage the participation of EV users in the V2G schemes.

The technical comparison between deploying V2G schemes and installing stationary storage to enhance city-scale load matching performance was presented in Section 3.4. Future studies should also compare the economic aspects of the two solutions. As previously mentioned, the V2G scheme deployment cost should consider the early EV battery replacement compensation for EV users.

### 4.2. On the optimal performance of renewable-powered city

It was shown in Section 3.1 that the load is positively correlated with the solar generation and anti-correlated with the wind generation on a diurnal basis. On the contrary, the load is positively correlated with wind generation and anti-correlated with solar generation on a seasonal basis. The right combination of wind and PV will maximize the load matching within the city. The results show that the optimal wind-PV electricity production share is 70% wind and 30% PV. It should be noted that the case study is for Sweden, where the load peaks during winter due to heating and lighting needs. In other regions, the seasonal peak load could occur during summer due to cooling needs. Thus, different geographical locations will most likely have different optimal wind-PV electricity production shares. However, the methods to define the optimal wind-PV electricity production share and RES-load ratio using SCSB in this study are universal, and they have also been applied in [40,53,55]. Optimal sizing using SCSB is recommended for studies on renewable-powered regional energy systems in various geographical locations.

The results in Section 3.2 showed that, based on SCSB performance, the net-zero energy city would only be the optimal scenario if V2G schemes were deployed. This highlights the importance of V2G schemes or energy storage in general to achieve the optimal performance of a renewable net-zero energy city. From the results in Section 3.4, it is shown that the net-zero energy city theoretically requires a massive stationary energy storage to achieve complete self-sufficiency. While it is theoretically possible to make the net-zero energy city self-sufficient, it will most likely be very costly to realize the scenario.

This study has focused on the technical aspects of a renewable-powered net-zero energy city considering EV flexibility. Studies on the economic and environmental aspects of the deployment of smart charging and V2G in renewable-powered net-zero energy cities are suggested for future research.

### 4.3. On the aggregated EV models for estimating energy system performance

The models in this paper are not intended for individual EV charging scheduling. Instead, they are intended to estimate the aggregated power dispatch in scenarios where smart charging and V2G schemes are deployed, as conducted in previous research [47,62]. From these aggregated power dispatch schemes, the performance of deploying smart charging and V2G in city-scale energy systems can be estimated without optimizing individual EV charging schedules, which takes significantly more time to compute.

Some simplifications with justifications were made in the paper. Setting the charging and discharging efficiency to 100% is one of them, as previously done in [80,81]. The assumption was used to keep the RES-load ratio fixed when comparing the three charging scenarios. When efficiency is less than 100%, the share of RES-load ratio for opportunistic charging, smart charging, and V2G will differ. In this case, the V2G scenario will have more load due to losses from round charging and discharging activities. That implies that to reach the net-zero energy city level, V2G schemes will require more electricity generation. The amount of extra generation required will depend on the frequency of V2G activation. If V2G is activated frequently, the city may require significant extra generation capacity to meet the demand. On the other hand, if V2G is only activated occasionally, the amount of extra generation required may be relatively small.

Additionally, the aggregated model has a slight drawback in handling the batteries as an aggregate as it assumes that the energy from the battery in one EV can be seamlessly transferred to another. The aggregated model only looks at the aggregated charging and discharging power, meaning that the overlapping part from the individual charging and V2G, i.e., the vehicle-to-vehicle (V2V) charging, is not modeled. It is justifiable when assuming no charging and discharging loss. In a more practical setting, the charging and discharging efficiency is less than 1 p.u. [82], and the aggregated model will fail to consider the loss due to the unmodeled V2V. Future studies may explore ways to understand and model the V2V and compensate for the loss in the aggregated model to improve accuracy.

## 5. Conclusions

This paper presents urban-scale energy matching optimization in a net-zero energy city powered by wind and solar energy, considering three EV charging scenarios: opportunistic charging, smart charging, and V2G. A city on the west coast of Sweden was used as a case study. Answering the research questions raised in this study, several conclusions based on the case study can be drawn:

1. Among all scenarios of EV charging schemes, wind-PV electricity production shares, and generation-load ratios, the optimal load matching performance is achieved in a net-zero energy city with V2G deployment and wind-PV electricity production share of 70:30.
2. In the optimal net-zero energy city, the load matching performance is increased from 68% in the opportunistic charging scenario to 73% in the smart charging scenario and to 84% in the V2G scenario.
3. When EV flexibility is fully utilized, a 2.4 GWh EV battery with V2G schemes as intermittent energy storage is equal to a 1.4 GWh stationary storage in terms of improving the urban-scale load matching performance.
4. Theoretically, it is possible to make the net-zero energy city 100% self-sufficient with 51.5, 50.4, and 49.0 GWh of stationary energy storage for the opportunistic charging, smart charging, and V2G scenarios, respectively. These numbers are considered massive compared to 8.1, 7.1, and 1.9 GWh required to reach 90% self-sufficiency in the respective charging scenarios.

The results from this paper show that there is a high potential from EV flexibility to improve energy system performance. Based on the findings of this study, several research topics are suggested for future studies. Future research suggestions include improving aggregated V2G models by taking into account V2V efficiency factors and developing probabilistic models of EV availability for grid purposes. This paper also suggests studies on optimal price signal modeling for V2G schemes in order to reach common technical and economic optima for EV owners, aggregators, and power system operators. Comprehensive economic and environmental assessments of V2G deployments in renewable-powered net-zero energy cities are also suggested for future studies.

## CRediT authorship contribution statement

**Reza Fachrizal:** Conceptualization, Data curation, Formal analysis, Methodology, Visualization, Writing – original draft. **Kun Qian:** Conceptualization, Data curation, Methodology, Software, Visualization, Writing – original draft. **Oskar Lindberg:** Data curation, Writing – review & editing. **Mahmoud Shepero:** Data curation, Methodology. **Rebecca Adam:** Supervision, Writing – review & editing. **Joakim Widén:** Supervision, Writing – review & editing. **Joakim Munkhammar:** Funding acquisition, Supervision, Writing – review & editing.

## Declaration of competing interest

The authors declare that they have no known competing financial interests or personal relationships that could have appeared to influence the work reported in this paper.

## Data availability

Data will be made available on request.

## Acknowledgments

This study was partly conducted within the research projects 'Increased utilisation of the grid with combined solar- and wind power parks' with grant number 49421-1, and 'Flexibility and energy efficiency in buildings with PV and EV charging' with grant number 50986-1, both funded by the Swedish Energy Agency, as well as 'PV parks as flexible resource in space and time' funded by the Åforsk Foundation, Sweden with grant number 23-397. This study also forms part of the Solar Electricity Research Center Sweden (SOLVE) and the Swedish strategic research programme StandUp for Energy. Kun Qian and Rebecca Adam were supported by the ZERO Emission Ports North Sea (ZEM Ports NS) Interreg project (number 38-2-8-19).

## References

[1] Edenhofer O, Pichs-Madruga R, Sokona Y, Farahani E, Kadner S, Seyboth K, Adler A, Baum I, Brunner S, Eickemeier P, Kriemann B, Savolainen J, Schlömer S, von Stechow C, Zwickel T, Minx J. Summary for policymakers. In: Climate change 2014: Mitigation of climate change. Contribution of working group III to the fifth assessment report of the intergovernmental panel on climate change. Cambridge, United Kingdom and New York, NY, USA: Cambridge University Press, IPCC; 2014, URL: https://www.ipcc.ch/site/assets/uploads/2018/02/ipcc_wg3_ar5_summary-for-policymakers.pdf.

[2] Koutra S, Becue V, Gallas M-a, Ioakimidis CS. Towards the development of a net-zero energy district evaluation approach : A review of sustainable approaches and assessment tools. Sustainable Cities Soc 2018;39(August 2017):784–800. http://dx.doi.org/10.1016/j.scs.2018.03.011.

[3] Komninos N. Net zero energy districts : Connected intelligence for carbon-neutral cities. Land 2022.

[4] Sakti AD, Ihsan KTN, Anggraini TS, Shabrina Z, Sasongko NA, Fachrizal R, Aziz M, Aryal J, Yuliarto B, Hadi PO, Wikantika K. Multi-criteria assessment for city-wide rooftop solar PV deployment: A case study of Bandung, Indonesia. Remote Sens 2022;14(12):2796. http://dx.doi.org/10.3390/rs14122796.

[5] International Energy Agency. Global EV outlook 2022 securing supplies for an electric future. Tech. rep., International Energy Agency; 2022, p. 221, URL: https://iea.blob.core.windows.net/assets/ad8fb04c-4f75-42fc-973a-6e54c8a4449a/GlobalElectricVehicleOutlook2022.pdf.

[6] Moro A, Lonza L. Electricity carbon intensity in European member states: Impacts on GHG emissions of electric vehicles. Transp Res D 2018;64(July 2017):5–14. http://dx.doi.org/10.1016/j.trd.2017.07.012.

[7] Fachrizal R, Lindberg O, Kinasih ADS, Muntean A, Widén J, Munkhammar J. Residential building with rooftop solar PV system, battery storage and electric vehicle charging: Environmental impact and energy matching assessments for a multi-family house in a Swedish city. In: 21st wind & solar integration workshop. Den Haag, the Netherlands: The Institution of Engineering and Technology (IET); 2022, p. 1–8.

[8] International Energy Agency. Global energy review 2019. Tech. rep., 2020, http://dx.doi.org/10.1787/90c8c125-en.

[9] Fachrizal R, Ramadhani UH, Munkhammar J, Widén J. Combined PV – EV hosting capacity assessment for a residential LV distribution grid with smart EV charging and PV curtailment. Sustain Energy Grids Netw 2021;26:100445. http://dx.doi.org/10.1016/j.segan.2021.100445.

[10] Khalid MR, Alam MS, Sarwar A, Asghar MSJ. A comprehensive review on electric vehicles charging infrastructures and their impacts on power-quality of the utility grid. eTransportation 2019;1:100006. http://dx.doi.org/10.1016/j.etran.2019.100006.

[11] Albadi MH, El-Saadany E. Overview of wind power intermittency impacts on power systems. Electr Power Syst Res 2010;80(6):627–32. http://dx.doi.org/10.1016/j.epsr.2009.10.035.

[12] Johansson S, Persson J, Lazarou S, Theocharis A. Investigation of the impact of large-scale integration of electric vehicles for a Swedish distribution network. Energies 2019;12(24). http://dx.doi.org/10.3390/en12244717.

[13] Guo C, Zhu K, Chen C, Xiao X. Characteristics and effect laws of the large-scale electric vehicle's charging load. eTransportation 2020;3:100049. http://dx.doi.org/10.1016/j.etran.2020.100049.

[14] Denholm P, O'Connell M, Brinkman G, Jorgenson J. Overgeneration from solar energy in California. A field guide to the duck chart. Tech. rep. November, National Renewable Energy Laboratory (NREL); 2015, http://dx.doi.org/10.2172/1226167.

[15] Dixon J, Bell K. Electric vehicles: battery capacity, charger power, access to charging and the impacts on distribution networks. eTransportation 2020;4:100059. http://dx.doi.org/10.1016/j.etran.2020.100059.

[16] Uski S, Forssén K, Shemeikka J. Sensitivity assessment of microgrid investment options to guarantee reliability of power supply in rural networks as an alternative to underground cabling. Energies 2018;11(10). http://dx.doi.org/10.3390/en11102831.

[17] Fachrizal R, Shepero M, van der Meer D, Munkhammar J, Widén J. Smart charging of electric vehicles considering photovoltaic power production and electricity consumption: a review. eTransportation 2020;4:100056. http://dx.doi.org/10.1016/j.etran.2020.100056, URL: https://linkinghub.elsevier.com/retrieve/pii/S2590116820300138.

[18] Lund H, Østergaard PA, Connolly D, Ridjan I, Mathiesen BV, Hvelplund F, Thellufsen JZ, Sorknses P. Energy storage and smart energy systems. Int J Sustain Energy Plan Manage 2016;11:3–14. http://dx.doi.org/10.5278/ijsepm.2016.11.2.

[19] Zhang L, Sun C, Cai G, Hai KL. Charging and discharging optimization strategy for electric vehicles considering elasticity demand response. eTransportation 2023;100262. http://dx.doi.org/10.1016/j.etran.2023.100262.

[20] Dixon J, Bukhsh W, Bell K, Brand C. Vehicle to grid: driver plug-in patterns, their impact on the cost and carbon of charging, and implications for system flexibility. eTransportation 2022;13:100180. http://dx.doi.org/10.1016/j.etran.2022.100180.

[21] Fachrizal R, Shepero M, Åberg M, Munkhammar J. Optimal PV-EV sizing at solar powered workplace charging stations with smart charging schemes considering self-consumption and self-sufficiency balance. Appl Energy 2022;307(August 2021):118139. http://dx.doi.org/10.1016/j.apenergy.2021.118139.

[22] Lindberg O, Lingfors D, Arnqvist J. Analyzing the mechanisms behind temporal correlation between power sources using frequency separated time scales: A Swedish case study on PV and wind. Energy 2022;259(July):124817. http://dx.doi.org/10.1016/j.energy.2022.124817.

[23] Jurasz J, Canales FA, Kies A, Guezgouz M, Beluco A. A review on the complementarity of renewable energy sources: Concept, metrics, application and future research directions. Sol Energy 2020;195(October 2019):703–24. http://dx.doi.org/10.1016/j.solener.2019.11.087, arXiv:1904.01667.

[24] Bistline JET, Blanford GJ. The role of the power sector in net-zero energy systems. Energy Clim Change 2021;2(May):100045. http://dx.doi.org/10.1016/j.egycc.2021.100045.

[25] Luthander R, Nilsson AM, Widén J, Åberg M. Graphical analysis of photovoltaic generation and load matching in buildings: A novel way of studying self-consumption and self-sufficiency. Appl Energy 2019;250(November 2018):748–59. http://dx.doi.org/10.1016/j.apenergy.2019.05.058.

[26] Doroudchi E, Alanne K, Okur O, Kyyrä J, Lehtonen M. Approaching net zero energy housing through integrated EV. Sustainable Cities Soc 2018;38(January):534–42. http://dx.doi.org/10.1016/j.scs.2018.01.042.

[27] Liu J, Zhou Y, Yang H, Wu H. Net-zero energy management and optimization of commercial building sectors with hybrid renewable energy systems integrated with energy storage of pumped hydro and hydrogen taxis. Appl Energy 2022;321(October 2021):119312. http://dx.doi.org/10.1016/j.apenergy.2022.119312.

[28] Stamatellos G, Zogou O, Stamatelos A. Energy analysis of a NZEB office building with rooftop pv installation: Exploitation of the employees ' electric vehicles battery storage. Energies 2022;15:6206.

[29] Ren H, Ma Z, Ming A, Fong L, Sun Y. Optimal deployment of distributed rooftop photovoltaic systems and batteries for achieving net-zero energy of electric bus transportation in high-density cities. Appl Energy 2022;319(December 2021):119274. http://dx.doi.org/10.1016/j.apenergy.2022.119274.

[30] Lopes RA, Martins J, Aelenei D, Lima CP. A cooperative net zero energy community to improve load matching. Renew Energy 2016;93. http://dx.doi.org/10.1016/j.renene.2016.02.044.

[31] Liu J, Zhou Y, Yang H, Wu H. Uncertainty energy planning of net-zero energy communities with peer-to-peer energy trading and green vehicle storage considering climate changes by 2050 with machine learning methods. Appl Energy 2022;321(December 2021):119394. http://dx.doi.org/10.1016/j.apenergy.2022.119394.

[32] Amado M, Poggi F, Amado AR, Breu S. A cellular approach to net-zero energy cities. Energies 2017;10:1826. http://dx.doi.org/10.3390/en10111826.

[33] Luthander R, Widén J, Nilsson D, Palm J. Photovoltaic self-consumption in buildings: A review. Appl Energy 2015;142:80–94. http://dx.doi.org/10.1016/j.apenergy.2014.12.028, URL: https://www.sciencedirect.com/science/article/pii/S0306261914012859.

[34] Balasubramanian S, Balachandra P. Effectiveness of demand response in achieving supply-demand matching in a renewables dominated electricity system: A modelling approach. Renew Sustain Energy Rev 2021;147(June):111245. http://dx.doi.org/10.1016/j.rser.2021.111245.

[35] Fachrizal R, Munkhammar J. Improved photovoltaic self-consumption in residential buildings with distributed and centralized smart charging of electric vehicles. Energies 2020;13(5). http://dx.doi.org/10.3390/en13051153.

[36] Bartolini A, Comodi G, Salvi D, Østergaard PA. Renewables self-consumption potential in districts with high penetration of electric vehicles. Energy 2020;213:118653. http://dx.doi.org/10.1016/j.energy.2020.118653.

[37] Mehrjerdi H, Hemmati R. Stochastic model for electric vehicle charging station integrated with wind energy. Sustain Energy Technol Assess 2020;37(November 2019):100577. http://dx.doi.org/10.1016/j.seta.2019.100577.

[38] Huang P, Munkhammar J, Fachrizal R, Lovati M, Zhang X, Sun Y. Comparative studies of EV fleet smart charging approaches for demand response in solar-powered building communities. Sustainable Cities Soc 2022;85(July):104094. http://dx.doi.org/10.1016/j.scs.2022.104094.

[39] Srithapon C, Månsson D. Predictive control and coordination for energy community flexibility with electric vehicles, heat pumps and thermal energy storage. Appl Energy 2023;347(December 2022):121500. http://dx.doi.org/10.1016/j.apenergy.2023.121500.

[40] Horak D, Hainoun A, Neugebauer G, Stoeglehner G. Battery electric vehicle energy demand in urban energy system modeling: A stochastic analysis of added flexibility for home charging and battery swapping stations. Sustain Energy Grids Netw 2023;111045. http://dx.doi.org/10.1016/j.segan.2023.101260.

[41] Zhang T, Chu CC, Gadh R. A two-tier energy management system for smart electric vehicle charging in UCLA: A solar-to-vehicle (S2V) case study. In: IEEE PES innov. smart grid technol. conf. eur.. Melbourne, Australia: IEEE; 2016, p. 288–93. http://dx.doi.org/10.1109/ISGT-Asia.2016.7796400.

[42] Van der Meer D, Mouli GRC, Mouli GME, Elizondo LR, Bauer P. Energy management system with PV power forecast to optimally charge EVs at the workplace. IEEE Trans Ind Inf 2018;14(1):311–20. http://dx.doi.org/10.1109/TII.2016.2634624.

[43] Li D, Zouma A, Liao J-t, Yang H-t. An energy management strategy with renewable energy and energy storage system for a large electric vehicle charging station. eTransportation 2020;6:100076. http://dx.doi.org/10.1016/j.etran.2020.100076.

[44] Modarresi Ghazvini A, Olamaei J. Optimal sizing of autonomous hybrid PV system with considerations for V2G parking lot as controllable load based on a heuristic optimization algorithm. Sol Energy 2019;184(March):30–9. http://dx.doi.org/10.1016/j.solener.2019.03.087.

[45] Edmunds C, Galloway S, Dixon J, Bukhsh W, Elders I. Hosting capacity assessment of heat pumps and optimised electric vehicle charging on low voltage networks. Appl Energy 2021;298(June):117093. http://dx.doi.org/10.1016/j.apenergy.2021.117093.

[46] Secchi M, Barchi G, Macii D, Petri D. Smart electric vehicles charging with centralised vehicle-to-grid capability for net-load variance minimisation under increasing EV and PV penetration levels. Sustain Energy Grids Netw 2023;35:101120. http://dx.doi.org/10.1016/j.segan.2023.101120.

[47] Heinisch V, Göransson L, Erlandsson R, Hodel H, Johnsson F, Odenberger M. Smart electric vehicle charging strategies for sectoral coupling in a city energy system. Appl Energy 2021;288(January). http://dx.doi.org/10.1016/j.apenergy.2021.116640.

[48] Dong Z, Zhang X, Zhang N, Kang C, Strbac G. A distributed robust control strategy for electric vehicles to enhance resilience in urban energy systems. Adv Appl Energy 2023;9(September 2022):100115. http://dx.doi.org/10.1016/j.adapen.2022.100115.

[49] Ledro M, Calearo L, Zepter JM, Gabderakhmanova T. Influence of realistic EV fleet response with power and energy controllers in an EV-wind virtual power plant. Sustain Energy Grids Netw 2022;31:100704. http://dx.doi.org/10.1016/j.segan.2022.100704.

[50] Fathabadi H. Novel wind powered electric vehicle charging station with vehicle-to-grid (V2G) connection capability. Energy Convers Manage 2017;136:229–39. http://dx.doi.org/10.1016/j.enconman.2016.12.045.

[51] Da Silva EC, Melgar-Dominguez OD, Romero R. Simultaneous distributed generation and electric vehicles hosting capacity assessment in electric distribution systems. IEEE Access 2021;9:110927–39. http://dx.doi.org/10.1109/ACCESS.2021.3102684.

[52] Bibak B, Tekiner-mogulkoc H. Influences of vehicle to grid (V2G) on power grid: An analysis by considering associated stochastic parameters explicitly. Sustain Energy Grids Netw 2021;26:100429. http://dx.doi.org/10.1016/j.segan.2020.100429, URL: https://doi.org/10.1016/j.segan.2020.100429.

[53] Peng Y, Ma X, Wang Y, Li M, Gao F, Zhou K, Aemixay V. Energy performance assessment of photovoltaic greenhouses in summer based on coupled optical-electrical-thermal models and plant growth requirements. Energy Convers Manage 2023;287(May):117086. http://dx.doi.org/10.1016/j.enconman.2023.117086.

[54] Amry Y, Elbouchikhi E, Le Gall F, Ghogho M, El Hani S. Optimal sizing and energy management strategy for EV workplace charging station considering PV and flywheel energy storage system. J Energy Storage 2023;62(November 2022):106937. http://dx.doi.org/10.1016/j.est.2023.106937.

[55] Qian K, Fachrizal R, Munkhammar J, Ebel T, Adam R. Validating and improving an aggregated EV model for energy systems evaluation. In: 2023 11th international conference on smart grid. IcSmartGrid, 2023, p. 1–7. http://dx.doi.org/10.1109/icSmartGrid58556.2023.10170794.

[56] Lin H, Bian C, Wang Y, Li H, Sun Q, Wallin F. Optimal planning of intra-city public charging stations. Energy 2022;238:121948. http://dx.doi.org/10.1016/j.energy.2021.121948.

[57] Lindberg O, Lingfors D, Arnqvist J, Meer DVD, Munkhammar J. Day-ahead probabilistic forecasting at a co-located wind and solar power park in Sweden: Trading and forecast verification. Adv Appl Energy 2023;9:100120. http://dx.doi.org/10.1016/j.adapen.2022.100120.

[58] Niveditha N, Singaravel MMR. Optimal sizing of hybrid PV – wind – battery storage system for net zero energy buildings to reduce grid burden. Appl Energy 2022;324(April):119713. http://dx.doi.org/10.1016/j.apenergy.2022.119713.

[59] Goldfarb D, Liu S. An O(n3L) primal interior point algorithm for convex quadratic programming. Math Program 1990;49(1):325–40. http://dx.doi.org/10.1007/BF01588795.

[60] Qian K, Fachrizal R, Munkhammar J, Ebel T, Adam RC. The impact of considering state-of-charge- dependent maximum charging powers on the optimal electric vehicle charging scheduling. IEEE Trans Transp Electrif 2023;9(3):4517–30. http://dx.doi.org/10.1109/TTE.2023.3245332.

[61] Basu A, Conforti M, Di Summa M, Jiang H. Complexity of branch-and-bound and cutting planes in mixed-integer optimization. Math Program 2023;198(1):787–810. http://dx.doi.org/10.1007/s10107-022-01789-5.

[62] González Vayá M, Baringo L, Krause T, Andersson G, Almeida PMR, Geth F, Rapoport S. EV aggregation models for different charging scenarios. In: 23rd international conference and exhibition on electricity distribution. CIRED, 2015.

[63] Luthander R. Self-consumption of photovoltaic electricity in residential buildings. 2018.

[64] Shepero M, Munkhammar J. Spatial Markov chain model for electric vehicle charging in cities using geographical information system (GIS) data. Appl Energy 2018;231:1089–99. http://dx.doi.org/10.1016/j.apenergy.2018.09.175, URL: https://www.sciencedirect.com/science/article/pii/S0306261918314922.

[65] SIKA. RES 2005 - 2006 the national travel survey. Technical report no. 2007:19, 2007, URL: www.sika-institute.se.

[66] Statista. 2022, URL: https://www.statista.com/forecasts/826586/car-ownership-in-sweden; [Online, accessed January 2023].

[67] Energy consumption of full electric vehicles cheatsheet - EV database. https://ev-database.org/cheatsheet/energy-consumption-electric-car.

[68] U.S. department of energy. 2022, URL: https://www.energy.gov/eere/electricvehicles/charging-home; [Online].

[69] Bi J, Wang Y, Sai Q, Ding C. Estimating remaining driving range of battery electric vehicles based on real-world data: A case study of Beijing, China. Energy 2019;169:833–43. http://dx.doi.org/10.1016/j.energy.2018.12.061, URL: https://www.sciencedirect.com/science/article/pii/S0360544218324277.

[70] Zine B, Bia H, Benmouna A, Becherif M, Iqbal M. Experimentally validated Coulomb counting method for battery state-of-charge estimation under variable current profiles. Energies 2022;15(21). http://dx.doi.org/10.3390/en15218172, URL: https://www.mdpi.com/1996-1073/15/21/8172.

[71] Meer DVD, Chao G, Munkhammar J. An alternative optimal strategy for stochastic model predictive control of a residential battery energy management system with solar photovoltaic. Appl Energy 2021;283(October 2020):116289. http://dx.doi.org/10.1016/j.apenergy.2020.116289.

[72] Casini M, Vicino A, Zanvettor GG. A receding horizon approach to peak power minimization for EV charging stations in the presence of uncertainty. Int J Electr Power Energy Syst 2021;126:106567.

[73] Capacity factor (net). 2021, URL: https://www.nrc.gov/reading-rm/basic-ref/glossary/capacity-factor-net.html; [Online].

[74] Wankmüller F, Thimmapuram PR, Gallagher KG, Botterud A. Impact of battery degradation on energy arbitrage revenue of grid-level energy storage. J Energy Storage 2017;10:56–66. http://dx.doi.org/10.1016/j.est.2016.12.004.

[75] Sarker MR, Murbach MD, Schwartz DT, Ortega-vazquez MA. Optimal operation of a battery energy storage system: Trade-off between grid economics and storage health. Electr Power Syst Res 2017;152:342–9. http://dx.doi.org/10.1016/j.epsr.2017.07.007.

[76] Niu J, Tian Z, Lu Y, Zhao H. Flexible dispatch of a building energy system using building thermal storage and battery energy storage. Appl Energy 2019;243(March):274–87. http://dx.doi.org/10.1016/j.apenergy.2019.03.187.

[77] Angenendt G, Zurmühlen S, Figgener J, Kairies K-p, Uwe D. Providing frequency control reserve with photovoltaic battery energy storage systems and power-to-heat coupling. Energy 2020;194:116923. http://dx.doi.org/10.1016/j.energy.2020.116923.

[78] Pasaoglu G, Fiorello D, Martino A, Zani L, Zubaryeva A, Thiel C. Travel patterns and the potential use of electric cars - results from a direct survey in six European countries. Technol Forecast Soc Change 2014;87:51–9. http://dx.doi.org/10.1016/j.techfore.2013.10.018.

[79] Guo J, Yang J, Lin Z, Serrano C, Cortes AM. Impact analysis of V2G services on EV battery degradation -a review. In: 2019 IEEE milan PowerTech. 2019, p. 1–6. http://dx.doi.org/10.1109/PTC.2019.8810982.

[80] Wang Q, Liu X, Du J, Kong F. Smart charging for electric vehicles: A survey from the algorithmic perspective. IEEE Commun Surv Tutor 2016;18(2):1500–17. http://dx.doi.org/10.1109/COMST.2016.2518628.

[81] Ahn C, Li C-T, Peng H. Optimal decentralized charging control algorithm for electrified vehicles connected to smart grid. J Power Sources 2011;196(23):10369–79. http://dx.doi.org/10.1016/j.jpowsour.2011.06.093, URL: https://www.sciencedirect.com/science/article/pii/S0378775311013309.

[82] Apostolaki-Iosifidou E, Codani P, Kempton W. Measurement of power loss during electric vehicle charging and discharging. Energy 2017;127:730–42. http://dx.doi.org/10.1016/j.energy.2017.03.015, URL: https://www.sciencedirect.com/science/article/pii/S0360544217303730.